



Cite this: *RSC Sustainability*, 2025, **3**, 4533

## Complete biodiverse lignocellulosic biomass fractionation process using the green solvent $\gamma$ -valerolactone

Moritz Schweiger, <sup>\*a</sup> Thomas Lang, <sup>a</sup> Eva Müller, <sup>a</sup> Vojtěch Jeřábek, <sup>b</sup> Jan Heyda, <sup>b</sup> Martin Klajmon, <sup>b</sup> Didier Touraud, <sup>a</sup> Magdalena Bendová, <sup>b</sup> Karel Řehák <sup>b</sup> and Werner Kunz <sup>a</sup>

Biomass pretreatment processes using organic solvents have historically been investigated for the separation of lignin from lignocellulosic biomass. This research explores how the pretreatment process can be expanded to fractionate all biomass components from various feedstock and waste streams and transform them into valuable bio-based molecules using green solvent mixtures and mild conditions. Using experimental and computational investigation techniques, this study further expands on the use of the green solvent  $\gamma$ -valerolactone (GVL) in biomass fractionation processes. Combining both results, a complete biodiverse process for the fractionation of all biopolymers in lignocellulosic biomass was achieved. This process yields lignin in native quality, very high purity and very high yield after a single extraction cycle at very mild conditions. Additionally, lignin-free cellulose in very high purity and yield, and hemicellulose degradation products in very high yield and purity, mainly xylose and glucose, can be separated during the process. These properties are essential for efficient valorization of the biopolymer products. The fractionation process proved to be similarly efficient in every step for different biomasses and waste-stream biomasses. GVL could be recovered and reused in every separation step and even be prepared from hemicellulose products, enabling a sustainable biomass dissolution cycle. This cycle stands as a basis for producing valuable biopolymer molecules, from biodiverse origin, that can be further converted into quality products for the chemical industry.

Received 18th July 2025  
Accepted 26th August 2025

DOI: 10.1039/d5su00600g  
[rsc.li/rscsus](http://rsc.li/rscsus)

### Sustainability spotlight

To achieve the replacement of fossil-based resources in the chemical industry by renewable and sustainable materials, the biodiverse, complete fractionation of lignocellulosic biomass into high purity biopolymer products with a green process is of great importance. Our interest was to develop a biomass fractionation process that can separate lignin, hemicellulose, and cellulose in an efficient way and in high yields and purities. We also used green solvents and mild fractionation conditions compared to existing processes. Furthermore, we validated the biodiversity of this process, making it applicable not only for high value lignocellulosic biomasses, but also for waste materials like wood sawdust, nutshells, or coffee silverskin. Our process aligns with the UN goals in responsible consumption and production (UN SDG 12).

## 1 Introduction

The primary goal of the chemical industry today is its transition towards renewable and sustainable resources. Currently, there is an enormous demand for fossil-based chemicals and their derived products, a demand that is projected to double over the next 25 years.<sup>1,2</sup> However, with the continuous depletion of fossil resources, future production will be unable to meet this rising demand. Therefore, it is crucial to identify and develop

alternative feedstocks that can replace fossil-based materials in the chemical industry. One such promising alternative is lignocellulosic biomass, with an estimated global annual production of 181.5 billion tons. This feedstock holds great potential due to its renewability, economic viability, and carbon neutrality.<sup>3</sup>

Lignocellulosic biomass encompasses renewable resources such as wood, plants, agricultural residues, grasses, and plant-based industrial waste streams like nutshells.<sup>4</sup> Despite its vast availability, only 8.2 billion tons are currently utilized,<sup>5</sup> primarily for livestock feed (61%), food (15%), and energy production (16%).<sup>2</sup> Traditionally, biomass has been used in the paper industry to produce cellulose fibers.<sup>3</sup> However, the concept of biorefineries, which seek to fully exploit the potential of lignocellulosic biomass, is gaining attraction due to the versatility of

<sup>a</sup>Faculty of Chemistry and Pharmacy, Department of Physical Chemistry II, University of Regensburg, Universitätsstraße 31, 93053 Regensburg, Germany. E-mail: moritz.schweiger@chemie.uni-regensburg.de

<sup>b</sup>Department of Physical Chemistry, University of Chemistry and Technology, Prague 6, CZ-16628, Czech Republic



the usable rawmaterials. These components could serve as precursors for producing sustainable energy,<sup>6</sup> biofuels,<sup>7</sup> bioplastics,<sup>8</sup> and various biochemicals,<sup>9</sup> such as amino acids,<sup>10</sup> platform chemicals like furfural,<sup>11</sup> or organic solvents like  $\gamma$ -valerolactone (GVL),<sup>12</sup> thereby offering a viable alternative to fossil-based chemical production. Nevertheless, several challenges must be addressed to fully realize the biorefinery concept, including reducing processing costs, improving process efficiency, ensuring the complete valorization of all biomass components, scaling up to industrial levels, and competing with the established fossil-based market.<sup>13</sup> This study highlights the improvements to a complete separation of all components of lignocellulosic biomass using green solvents compared to existing processes. With the green solvent GVL, complete lignocellulosic biomass fractionation can be achieved through a simple, mild, and optimized process, which greatly improves upon existing biomass fractionation processes in terms of biopolymer yield, purity and quality, and process conditions.

Lignocellulosic biomass consists mainly of cellulose (44%), hemicellulose (28%), and lignin (20%), with smaller fractions of proteins, other extractives (6%), and ash (2%). The overall structures of these three main biopolymers are depicted in Fig. (1).<sup>14,15</sup>

Hemicellulose is a heterogeneous polysaccharide primarily composed of xylose and glucose backbones, with varying pentose or hexose substituents depending on the biomass type.<sup>16–21</sup> In this study, the degradation products of hemicellulose, particularly xylose, are being dissolved and separated from other biomass extractives. Xylose can act as a precursor for important platform chemicals in the future.<sup>22</sup> Cellulose, a polysaccharide from glucose, can be efficiently separated from lignin and hemicellulose and be recovered in high purity to enable further processing. Lignin is a complex, three-dimensional heteropolymer. It is composed mainly of the

aromatic monomers sinapyl alcohol, coniferyl alcohol, and *p*-coumaryl alcohol, which are interconnected by ether and carbon–carbon linkages. These monomers form the corresponding subunits syringyl (S), guaiacyl (G), and hydroxyphenyl (H). The monomers can bond through carbon–carbon linkages, including  $\beta$ - $\beta'$ ,  $\beta$ -1', and 5-5', or through carbon–oxygen bonds, such as  $\beta$ -O-4',  $\alpha$ -O-4', and 4-O-5' linkages, varying on the biomass source.<sup>23–39</sup> Lignin in biomass is typically present in lignin–carbohydrate complexes with hemicellulose, enabling their co-extraction.<sup>23</sup> While lignin is currently mostly burned to recover process energy in the paper industry,<sup>3</sup> it has potential for a variety of applications, such as UV-protective films,<sup>30–32</sup> antioxidant additives,<sup>33,34</sup> fragrance monomers,<sup>35</sup> medical uses<sup>36</sup> or vanillin production.<sup>37,38</sup>

With an effective separation of lignin in maximally natural constitution with its native ether content comes the fractionation of all biopolymers in high yields and quality. This was done through the combination of well-established extraction methods, namely organosolv processes<sup>39,40</sup> and aldehyde-assisted processes to prohibit extensive lignin condensation reactions.<sup>41</sup> Since GVL/water mixtures have shown good lignin solubility already in the past,<sup>39</sup> we also investigated the performance of the GVL/water solvent system by means of advanced computational techniques, namely, the quantum-mechanics-aided COSMO-SAC model and atomistic molecular simulations, to provide further theoretical insights into the behavior of the proposed fractionation media. Both experimental and simulation results led to a further understanding of the potential of GVL in biomass fractionation, not only due to its nature as a green solvent,<sup>42–44</sup> but also its potential to be produced efficiently from biobased resources.<sup>45–50</sup> Given GVL's ability to dissolve lignin<sup>51</sup> and hemicellulose<sup>52</sup> in substantial quantities, and its prospect to improve cellulose dissolution,<sup>53</sup> it was considered an ideal solvent for this study. Additionally, GVL

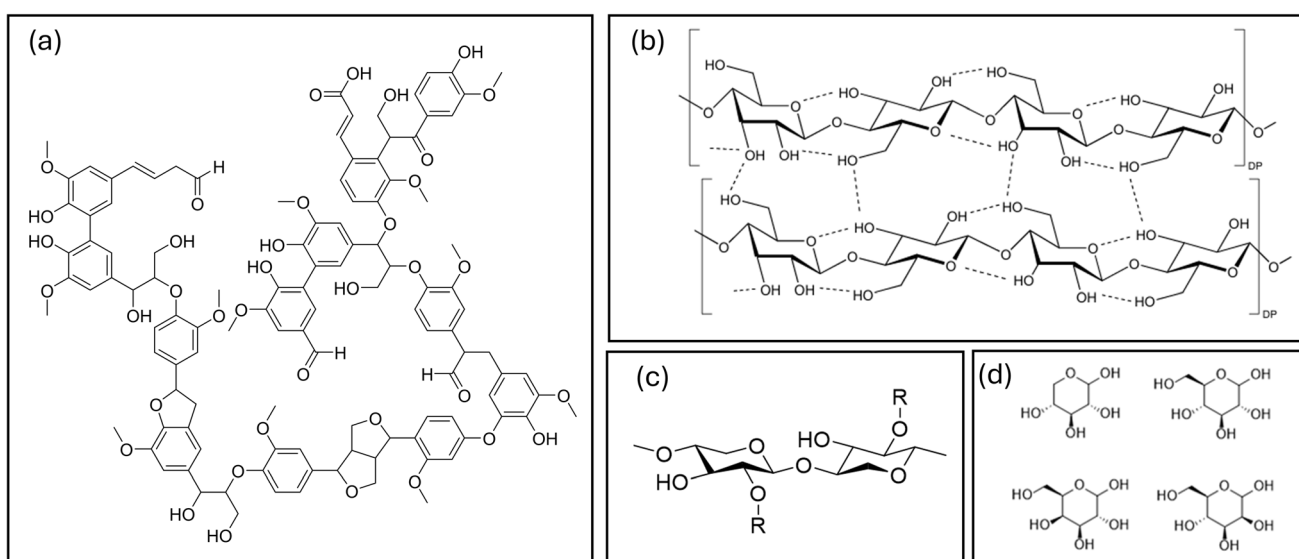


Fig. 1 (a) Structural excerpt of lignin. (b) Structural excerpt of cellulose chains with intermolecular and intramolecular hydrogen bonding. (c) Structural excerpt of hemicellulose. (d) Possible monomeric sugar molecules that can be part of the substituted hemicellulose backbone in place of R.



can be easily recycled through simple distillation techniques<sup>54</sup> or CO<sub>2</sub> extraction.<sup>55</sup> Summarizing all results, we designed an efficient process for complete biodiverse biomass fractionation using mainly GVL, yielding cellulose, lignin and hemicellulose products with high value for further processing, all in one efficient and mild extraction cycle.

It is very important to clarify the several problems of other fractionation processes in existing literature, which our process greatly improves upon. A common approach is the use of ionic liquids (IL's) to dissolve biomass components and fractionate them. IL's are mainly organic salts with melting points <100 °C. They provide advantages such as low volatility, high thermal stability, and high adaptability to certain processes due to the large number of possible combinations of cations and anions. IL's mainly disrupt the intermolecular hydrogen bonds between biopolymers, facilitating their fractionation and dissolution.<sup>56</sup> Examples for IL's being developed for biomass fractionation are especially imidazolium-based IL's like 1-ethyl-3-methylimidazolium acetate<sup>57</sup> or 1-butyl-3-methylimidazolium acetate.<sup>58</sup> These IL's have high cost and toxicity, and do not show complete fractionation ability of all biopolymers.<sup>57,58</sup> Protic IL's such as triethylammonium hydrogen sulfate dissolved up to 85% lignin and 100% hemicellulose from *Miscanthus x giganteus* with low production cost and high recovery. Still, the purity and quality of the extracted biopolymers was not yet efficient enough for industrial application.<sup>59</sup> Other general problems of using IL's for biomass fractionation are their high costs, potential toxicity, and difficult recovery.<sup>56,60</sup> A better alternative to IL's are deep eutectic solvents (DES). DES are mainly formed by mixing a hydrogen bond accepting and a hydrogen bond donating component, resulting in a mixture with a melting point lower than that of the individual components. DES are generally considered more biodegradable, less toxic, and more cost-efficient than IL's.<sup>59,61</sup> Several DES formulations have been developed to fractionate biomass. A choline chloride/oxalic acid DES showed medium delignification capabilities from wheat straw of 57.9% lignin removal. This process allows a breakdown of the lignin structure, but struggles with further processing cellulose into valuable products, while fully removing lignin and hemicellulose from the biomass.<sup>62</sup> A DES based on choline chloride/levulinic acid could effectively fractionate cellulose (3% lignin left), lignin, and hemicellulose from acacia wood at high temperatures of 160 °C, still being very energy-intensive and the lignin being of very poor quality, meaning high condensation and low purity due to cellulose/hemicellulose breakdown products.<sup>63</sup> Other DES, or natural deep eutectic solvents (NADES), based on lactic acid,<sup>64</sup> or three components DES, with additional protection agents like ethylene glycol, that ensure an uncondensed state of lignin<sup>65</sup> also yielded great results for biomass fractionation, yet still struggle with DES recovery, high temperatures up to 160 °C, recovery of the hemicellulose component, biodiversity, and long reaction times up to 24 hours. DES provide clear advantages compared to IL's in lignin separation and subsequent complete biomass fractionation but are not yet effective enough for industrial application.<sup>56,61,65</sup> A last possibility is the use of organosolv processes to fractionate biomass. This method has

been highly developed, with the use of different organic solvents like ethanol, methanol or acetone in combination with water and other catalysts/additives to solubilize lignin and hemicellulose, leaving behind a pure cellulose residue. Core mechanisms are the disruption of lignin-hemicellulose complexes due to slightly acidic conditions, and the dissolution of lignin and hemicellulose fragments through the organic solvents. While pathways to efficiently separate lignin, hemicellulose, and cellulose have been found, problems like solvent toxicity, energy-intensive and solvent-intensive process conditions, lack of biodiversity, or unsatisfactory quality of biopolymer products still reside.<sup>66,67</sup> While simple mixtures of acidic organic solvent/water mostly extract lignin in high quantities, elevated temperatures are necessary due to the condensation of lignin during the process, leading to lower value products. Additionally, many organic solvents pose the risk of flammability or other safety/environmental risks due to their high volatility.<sup>68–70</sup> GVL has proven to be an excellent option for organosolv processes due to its advantageous properties,<sup>67</sup> with its large-scale availability increasing significantly over the next few years. Due to additives that can reduce lignin condensation and thus fractionate all biopolymers at relatively low temperatures below 100 °C, GVL could be industrially used in the future. The challenge of designing a process using the advantages of GVL combined with simple solvent recovery, low process temperatures, low solvent quantities, high biopolymer yields and purities, high lignin quality, low extraction times, and especially biodiversity of the process has been developed in the frame of this work. This process improves greatly upon various problems of existing biomass fractionation processes. Through experimental and computational methods, the potential of GVL as the optimal solvent for biomass fractionation was validated. Cellulose, lignin and hemicellulose were then extracted from biomass using mild GVL extraction processes and the process efficiency was analyzed by fractionation yield and purity. The differences between a default extraction process with GVL and the improved aldehyde-assisted GVL extraction process were examined qualitatively to show how efficient lignin removal enables complete biopolymer fractionation. In a concluding remark, it was shown how the process in this study greatly improves upon existing processes in literature. The extractives from all three biopolymers can be considered for further applications, as pathways for specific applications were developed, which will also be specifically addressed in future research following up on this article.

## 2 Materials and methods

### 2.1 Chemicals and materials

Sulfuric acid (95–98%, CAS 7664-93-9), L-cysteine (98%, CAS 52-90-4), DMSO-d6 (99.8%, CAS 2206-27-1), acetaldehyde (for synthesis, CAS 75-07-0), acetone (>99.5%, CAS 67-64-1), dimethyl sulfoxide (DMSO) (for analysis, CAS 67-68-5), 1,4-dioxane (for analysis, CAS 123-91-1), ethanol (for analysis, CAS 64-17-5), ethyl acetate (for analysis, CAS 141-78-6), *para*-formaldehyde (37% in water, CAS 50-00-0), hydrochloric acid (37%, CAS 7647-01-0), methanol (for analysis, CAS 67-56-1), toluene



(for analysis, CAS 108-88-3), sodium hydroxide (for analysis, CAS 1310-73-2), propionic aldehyde (>98%, CAS 123-38-6), were purchased from Merck KGaA (Darmstadt, Germany).

$\gamma$ -Valerolactone (GVL) (anal. Grade, CAS 108-29-2) was provided by KVT-Technology/Glaconchemie (Graz, Austria).

*n*-Hexane (>99%, CAS 110-54-3), *n*-heptane (>99%, CAS 142-82-5), methyl-tetrahydrofuran (>99%, CAS 96-47-9) were purchased from Fisher Scientific GmbH (Schwerte, Germany).

Sodium hydrogen carbonate (>99.5%, CAS 144-55-8) was purchased from Carl Roth GmbH & Co. KG (Karlsruhe, Germany).

Millipore distilled water was cleaned in a Millipore purification system (electrical conductivity  $p > 18 \text{ M}\Omega\text{cm}$ ).

Peanut shells and skin were removed from store bought peanuts; pistachio shells were removed from store bought pistachios; hazelnut shells were removed from store bought hazelnuts. Walnut shells were removed from home grown walnuts.

Coffee silverskin was provided by Rheorik Rösterei & Feinkost GmbH (Regensburg, Germany).

Birch sawdust and Beech sawdust were provided by Schreinerei Heitzner (Traitsching, Germany).

Cashew shell powder was provided by Orpia-Innovation (Paris, France).

Almond shells were provided by Otto A. Müller Recycling GmbH (Ahrensburg, Germany).

Spruce sawdust was provided by HCR Holz Centrum Regensburg GmbH (Regensburg, Germany).

## 2.2 Lignin and hemicellulose extraction process

The default lignin extraction follows a method established by Cheng *et al.*<sup>39</sup> Using GVL/water mixtures as extraction solvent, the optimum extraction parameters were determined through variation in temperature, solid loading, extraction time, solvent composition and pH value. Biomass samples were dried at 75 °C for 48 h to remove water residues, then milled into powder with a diameter of 2 mm. An amount of 9 g of the milled biomass powder was transferred into a 250 mL round flask. To the flask, 90 mL of a GVL/water (9/1 wt/wt) mixture were added. The mixture was subjected to ultrasonic treatment for 30 min at 60 °C to achieve optimal swelling of the lignocellulose structure, enabling a good solvent penetration for the extraction. A concentration of 0.075 mol L<sup>-1</sup> sulfuric acid was set in the mixture. The round flask was equipped with a magnetic stirring bar and subjected into an oil bath at 120 °C for 2 h under continuous stirring. These optimum conditions for the GVL-based organosolv process were determined by variation of solid loading, acid concentration, solvent composition, extraction time, and reaction temperature to maximize yield and purity of the extracted lignin (details see SI Section S1). After the extraction finished, the round flask was air-cooled to room temperature before being put in an ice bath for 20 min to prohibit intense condensation reactions. Residual biomass residue, mostly cellulose, was removed through a Buchner filter from the lignin/hemicellulose/GVL/water solution. The filter cake was washed with 15 mL of GVL and 15 mL of water three times each. The

filtrate was collected in an appropriate beaker and subjected to 10 times its volume of water to precipitate the lignin. The lignin was collected through centrifugation at 4000 rpm for 15 min. The residual solution was subjected to vacuum distillation at 60 °C and 0.001 bar to completely remove the solvent mixture and collect the hemicellulose residues. The solid lignin was washed with distilled water multiple times to remove GVL and hemicellulose residues (which were in the end added to the hemicellulose fraction) and then dried at 75 °C for 48 h in a drying oven, then for 24 h in a vacuum desiccator equipped with silica gel. Finally, light brown colored lignin powder was obtained. The color varied for different biomass sources.

Each biomass sample underwent three separate extraction steps to ensure nearly complete lignin extraction. The lignin yield was calculated through eqn (1).

$$\text{Yield} = \frac{m_{\text{extracted lignin}}}{m_{\text{biomass}} \times \text{lignin content}} \times 100 \quad (1)$$

Following this, the purity of the extracted lignin was assessed using a modified version of the CASA method, see Section 2.6.2.

## 2.3 Aldehyde assisted extraction process

The modified extraction method of lignin and hemicellulose is based on the aldehyde-assisted fractionation established by Lan *et al.* (2018).<sup>41</sup> The method was optimized for our extraction process using GVL by varying temperature, extraction time, acid content, water content, and neutralization method (for details see SI Section S2).

5 g of biomass, 27.5 mL of GVL, 5.3 mL of propionaldehyde, and 0.94 mL of 37% HCl solution (instead of sulfuric acid, details see SI) were added into a 100 mL glass flask containing a 20 mm PTFE-coated stir bar. After connecting the flask to a reflux condenser, the mixture was heated to 85 °C for 3 h (heat up time included). To ensure ideal stirring during the reaction, the stirrer was turned on 15 min into the reaction and was set to approx. 400 rpm. After completion of the extraction, the flask was set aside until it cooled down to room temperature. The mixture was filtered using a Buchner funnel and washed with 5 × 5 mL GVL and 2 × 10 mL methanol (important for neutralization, see SI Section S2). The collected cellulose was set aside. The filtrate was neutralized by adding 1.7 g of NaHCO<sub>3</sub> and stirred for approx. 1 h at room temperature. After neutralization residual NaHCO<sub>3</sub> and resulting NaCl were filtered using a Buchner funnel. Neutralization was necessary to avoid deprotection and recondensation during lignin recovery. GVL from the neutralized filtrate was evaporated by using a vacuum distillation setup (1 × 10<sup>-3</sup> bar, 60 °C). The resulting slurry was redissolved in 10 mL ethyl acetate until it was not viscous anymore. Lignin was precipitated by slowly pipetting one part (volume) of the prepared solution to 10 parts of vigorously stirring heptane. The stirring was stopped after the residue was disaggregated, and the yellow-colored supernatant was decanted into an Erlenmeyer flask. The remaining lignin-rich residue was solidified by adding 20 mL of distilled water to the gel-like residue. The residue was filtered using a Buchner funnel and washed with 2 × 10 mL distilled water. The



recovered lignin was dried overnight using a desiccator. The resulting lignin powder was purified using the following procedure: 10 mL diethyl ether (see SI, Section S2) were added to the lignin powder and placed into an ultrasonic bath. The yellow-colored supernatant liquid was decanted through a fritted filter funnel (pore size: G3) and added to the hemicellulose fraction. The purification process was repeated one more time. The resulting lignin was dried at 40 °C for 1 h and stored in a closed container. The depolymerized hemicellulose from the heptane/ethyl acetate filtrate and the washing step was received by distillation using a rotary evaporator.

The heptane/ethyl acetate solvent mixture was used instead of water for precipitation of the lignin to reduce the overall solvent consumption from a total of 322.5 mL of solvents in the default extraction process to 197.5 mL of solvents in the aldehyde assisted extraction process. Moreover, the high enthalpy of vaporization for water could be avoided, and easily vaporizable *n*-heptane could reduce the distillation energy needed. Still, aqueous precipitation can be used in this process if a complete set of green solvents is necessary.

The theoretical lignin extraction yield was calculated by using eqn (1) to further calculate the actual lignin extraction yield, as the introduction of protecting groups altered the molecular weight of lignin structures. This was suggested by Ian *et al.* (2019).<sup>71</sup>

$$\text{Yield} = m_{\text{biomass}} \times \text{LC} \times \left[ \left( \frac{236}{196} \times \%G + \frac{266}{226} \times \%S \right) \times \text{EC} + (1 - \text{EC}) \right] \quad (2)$$

In eqn (2), *m* means weight of biomass subjected to extraction, LC means lignin content in the biomass, %G/%S means percentage of guaiacyl/syringyl units present in lignin, and EC means the ether content. S/G-ratio and ether content are determined by 2D HSQC NMR spectroscopy. The molecular weights of the β-O-4 bonded monomeric units in native lignin are 196 g mol<sup>-1</sup> for a G unit and 226 g mol<sup>-1</sup> for an S unit. Following protection with propionaldehyde, these molecular weights increase to 236 g mol<sup>-1</sup> for G and 266 g mol<sup>-1</sup> for S.

A comparison for the process parameters for both extraction processes is shown in SI Section S7.

#### 2.4 Solvent recovery process

Solvents from all mixtures containing GVL could be recovered for solvent reusability. GVL was recovered through simple vacuum distillation at 60 °C and 10<sup>-3</sup> bar. Water can be separated from GVL through rotary vacuum evaporation at 40 °C and 0.1 bar. Similarly, ethyl acetate (50 °C, 0.150 bar) and heptane (50 °C, 0.07 bar) can be separated and reused for lignin precipitation after rotary vacuum evaporation.

#### 2.5 NMR spectroscopy

NMR experiments were conducted using an Avance III HD 400 spectrometer (400.13 MHz Proton, 5 mm BBO 400 SB BB-H-D sample head with Z-gradient). Lignin samples were dissolved in DMSO-*d*<sub>6</sub> at 60 mg mL<sup>-1</sup> and transferred to NMR glass tubes

after complete dissolution. For all samples, 1H-NMR and 2D-HSQC-NMR spectra were measured to evaluate the S/G-ratio and the ether content of lignin from different biomass sources to accurately calculate lignin yields through eqn (1). For lignin from the aldehyde extraction process, the protection rate can also be calculated through 2D-HSQC-NMR. SpinWorks was used to analyze the NMR spectra. The detailed NMR assignment method can be found in SI Section S3.

#### 2.6 UV/vis spectroscopy

**2.6.1 Spectroscopy.** UV/vis spectroscopy experiments were conducted on a double-beam UV/vis spectrophotometer from PerkinElmer Lambda 19 UV/Vis/NIR (Dordau, Germany). Examined samples were measured in micro-UV cuvettes with an optical path length (L) of 1 cm from brand GmbH & Co.KG (Wertheim, Germany) against a reference sample at 25 °C in a wavelength range from 200 nm to 400 nm.

**2.6.2 CASA lignin content and purity determination.** In all biomass samples, the lignin content was determined through the Cysteine Assisted Sulfuric Acid (CASA) method, which was first described by Lu *et al.* (2021).<sup>72</sup> A stock solution of 0.1 g mL<sup>-1</sup> L-cysteine in 72% sulfuric acid was prepared. In 1 mL of stock solution, 20 mg of a ground biomass sample (*m*) were dissolved under stirring at room temperature, before being diluted to 100 mL (V) with distilled water. The UV/vis absorbance (*A*<sub>283,biomass</sub>) was measured at 283 nm to determine the overall lignin content using eqn (3) with a molar absorption coefficient *ε* of 17.25 L g<sup>-1</sup> cm<sup>-1</sup>. The lignin content can be overestimated due to other aromatic extractives from proteins, but this is generally negligible due to their very low content.

$$\text{Lignin content [\%]} = \frac{A_{283,\text{biomass}} \times V}{\epsilon \times L \times m} \times 100 \quad (3)$$

Additionally, the lignin purity could be determined by using a modification of the CASA method, which was validated internally. The loss of lignin in a representative biomass sample modeled with extracted lignin was measured, which correlated to the purity of the extracted lignin sample. To this end, instead of biomass, an equivalent amount of extracted lignin to the lignin content in the respective biomass (e.g. 1 g biomass, 20% lignin content → 0.2 g extracted lignin) was dissolved in 1 mL stock solution and diluted to 100 mL with distilled water. Eqn (4) was used to calculate the lignin purity by dividing the absorbance of the extracted lignin sample (*A*<sub>283</sub>) by the absorbance of the respective biomass sample (*A*<sub>283,biomass</sub>). Since aromatic parts from proteins are also removed during extraction, the lignin purity can be underestimated.

$$\text{Lignin purity [\%]} = \frac{A_{283}}{A_{283,\text{biomass}}} \times 100 \quad (4)$$

#### 2.7 Carbohydrate content determination

The hemicellulose and cellulose contents for different biomasses were determined using a simple acid hydrolysis method, since the lignin content was already determined



through UV/vis spectroscopy. The biomass sample was dried in an oven at 105 °C for 15 h to remove residual moisture. Of the dried biomass, 1 g was subjected in a round flask to 100 mL of a neutral detergent solution containing sodium lauryl sulfate (30 g L<sup>-1</sup>) and EDTA (20 g L<sup>-1</sup>) to remove extractives like proteins, lipids, and other non-fiber components. The gravimetric difference determined the extractive content. After filtering and drying, the residual biomass was subjected to 100 mL of 1 mol L<sup>-1</sup> sulfuric acid at 100 °C for 2 h to hydrolyze hemicellulose into water-soluble sugar molecules. After filtering and drying the residual biomass at 105 °C for 15 h, it was weighed. The gravimetric difference determined the hemicellulose content of a certain biomass. Due to the known lignin content, the cellulose content was determined by subtracting the overall lignin content from the residual weight of the biomass after extractive and hemicellulose removal.

## 2.8 Gas chromatography coupled with mass spectrometry

Qualitative analysis was carried out using GC-MS with an Agilent 7890B GC system, fitted with a ZB-5MSplus column, and a Jeol AccuTOF GCX mass spectrometer. Samples (1  $\mu$ L) were injected using an autosampler in split mode (split ratio 75 : 1) at an injection temperature of 300 °C. The septum purge flow was maintained at 3 mL min<sup>-1</sup>. The column temperature was initially set at 40 °C for 3 minutes, then ramped to 100 °C at 30 °C min<sup>-1</sup>, followed by a further increase to 300 °C at 40 °C min<sup>-1</sup>, where it was held for 5 minutes. Molecules were identified by comparison with the NIST MS Search 2.2 database.

## 2.9 Computational and simulation methods

For the purposes of computational investigations conducted within this study, we developed a model organosolv lignin oligomer. It consists of five *p*-coumaryl alcohol (PCA has proven to be a suitable building block for this purpose in previous research<sup>73,74</sup>) units connected by three  $\beta$ -O-4' and one  $\beta$ -5' linkages, reflecting a typical distribution of linkages in most wood-based biomasses (determined through 2D-HSQC-NMR, details see SI Section S3). This pentamer is hereafter denoted "PCA-5mer" and its molecular topology can be found in the SI Section S6.

**2.9.1 COSMO-SAC.** To examine the thermodynamic behavior of PCA-5mer/solvent(s) systems, the conductor-like screening model-segment activity coefficient (COSMO-SAC) model<sup>75–77</sup> was employed. COSMO-SAC is an advanced, strictly predictive model that combines quantum-mechanical (QM) calculations and a statistical approach to estimate macroscopic thermodynamic properties of solutions, such as the activity coefficients ( $\ln \gamma_i$ ) of individual solution components and, hence, phase equilibria including miscibility and solubility. In this framework, QM density functional theory (DFT) calculations within a continuum solvation model are used to generate the molecular surface screening charge density,  $\sigma$ , which is then transformed into the  $\sigma$ -profile, a histogram representing the amount of molecular surface area as a function of  $\sigma$ . The  $\sigma$ -profiles of the involved molecular species are subsequently used in a statistical model to estimate solution properties. As such,

COSMO-based models rely solely on molecular structure as input and do not require auxiliary solution-specific data. Therefore, they provide an efficient tool for solvent screening and ranking (based on predicted phase equilibria or  $\ln \gamma_i$ ) across various fields, including (bio)polymer systems.<sup>73,78–80</sup>

In this work, we applied the revised, open-source COSMO-SAC implementation,<sup>77</sup> specifically the COSMO-SAC-2010 variant.<sup>78</sup> Although several applications of other COSMO-based models and implementations to biopolymer-based systems exist,<sup>73,74,78,81–84</sup> to the best of our knowledge, the present study represents the first application of this open-source COSMO-SAC implementation in this field.

The molecular  $\sigma$ -profile database distributed with the COSMO-SAC package<sup>77</sup> did not cover all the compounds we intended to include. Therefore, for the sake of consistency, we determined the  $\sigma$ -profiles *de novo* for all solvents and lignin solutes considered in this study, not just the missing ones. This was based on QM calculations of molecular surface screening charge densities using Gaussian 16 software<sup>85</sup> at the BP86/TZVP level with the conductor-like polarizable continuum model (C-PCM)<sup>86</sup> for the solvation. The initial molecular geometries of solvents were generated from SMILES codes using the sophisticated ETKDGv3 method,<sup>87</sup> refined at a molecular-mechanical level<sup>88</sup> (both using the RDKit package<sup>89</sup>), and subsequently optimized quantum-mechanically at BP86/TZVP/C-PCM in Gaussian. For the solute PCA-5mer, its geometry was taken directly from the final snapshot (at 100 ns) of an MD simulation of the PCA-5mer/GVL system (for details, see the following section) to reflect a realistic liquid-phase conformation. The geometry was used without further refinement. In principle, oligomers – and even smaller oligomers – can adopt numerous conformers. However, we demonstrate in Section S4 of the SI that the specific geometry of PCA-5mer has a limited impact on qualitative solvent screening. The  $\sigma$ -profiles and corresponding geometries of all molecular species considered in this study are provided as part of the SI.

In the computational study, we used the activity coefficient of the solute PCA-5mer at infinite dilution in solvents ( $\ln \gamma_{\text{PCA-5mer}}^\infty$ ), as predicted by COSMO-SAC, to assess PCA-5mer-/solvent thermodynamic affinity in the liquid phase (that is, the ability of solvents to dissolve this lignin model), following previous studies.<sup>73,74,78</sup> For poorly soluble species, the mole fraction solubility and the activity coefficient are interrelated by the following proportion:  $x_i^{\text{sat}} \propto 1/\gamma_i^\infty$ . As a result, low  $\ln \gamma_i$  values indicate higher solute–solvent affinity and tendency to solubilize the solute, and *vice versa*. Comparing predicted  $\ln \gamma_{\text{PCA-5mer}}^\infty$  values across different solvents thus enabled an evaluation of their dissolving efficiency.

**2.9.2 MD simulations.** Simulations of PCA-5mer in water, GVL, and their 50 mol% mixture were performed in GROMACS simulation package, utilizing TIP4P/2005 water model and GAFF parameterizations (with ESP partial charges) of GVL and PCA-5mer derived according to recommended protocol.<sup>90–94</sup> We note that GVL dipole on carbonyl group was increased by *ca* 10% and sigma of atoms adjusted to quantitatively reproduce water-GVL miscibility and experimental density of pure GVL and 50 mol% mixture. Simulations were performed in



isothermal-isobaric (NpT) ensemble at standard temperature (298 K) and pressure (1 bar), which were controlled by V-rescale thermostat ( $\tau_T = 0.5$  ps) and C-rescale barostat ( $\tau_p = 2.0$  ps).<sup>95,96</sup> LINCS algorithm was used to constrain all bonds involving hydrogen atoms.<sup>97</sup> 1 nm cut-off was used for short range Lennard-Jones and electrostatics. The Particle mesh Ewald (PME) method on a 0.16 nm grid accounted for long-range electrostatics.<sup>98</sup> Studied systems consisted of a single PCA-5mer molecule, 4181 water, 800 GVL (pure solvents), or 664 water and 664 GVL molecules (equimolar mixture), which were randomly distributed in the simulation box by PACKMOL software.<sup>99</sup> After minimization and short equilibration, the system reached equilibrium size of *ca*  $5 \times 5 \times 5$  nm<sup>3</sup> and was propagated with 2 fs time-step (leap-frog integrator) and 1 ps sampling frequency for 100 ns, resulting in 100 000 configurations for data analysis. Solution structure in the vicinity of a fully flexible PCA-5mer molecule was analyzed with group-specific proximal (1D) resolution. The spatial (3D) resolution was applied to rigid compact and extended conformations, which represent dominant structures as sampled in water and in GVL respectively. In-house codes were utilized, and the results are compared between neat solvents and solvent mixture.<sup>100</sup>

### 3 Results and discussion

#### 3.1 GVL-water system as optimal solvent mixture for lignin extraction

The effective extraction of lignin from lignocellulosic biomass is a core step in achieving high quality fractionation in our process. Multiple experimental observations indicate that GVL/water mixed solvent exhibits remarkably efficient behavior in terms of lignin dissolution.<sup>39,40,51</sup> Together with the green and renewable nature of GVL, this solvent mixture appears to be optimal for the fractionation of lignocellulosic biomass. Therefore, we applied the COSMO-SAC thermodynamic model

and MD simulations to support understanding of and provide insight into the behavior of the GVL/water mixture, also in the context of other (not necessarily green) solvents. Additionally, the interaction of the solvent mixture with PCA-5mer, a lignin model molecule, was investigated. This should underline the mechanistic effectiveness of GVL in GVL/water mixtures at the solubilization of lignin, while profiting from the green properties of the solvent. Overall, this chapter gives arguments supporting our selection of GVL as the main solvent for our biomass fractionation process.

**3.1.1 COSMO-SAC screening calculations.** First, COSMO-SAC was applied to *a priori* predict the limiting activity coefficients of the solute PCA-5mer in a range of pure solvents, including conventional, toxic, hazardous, and novel green alternatives, with the goal of assessing the relative performance of GVL compared to other pure solvents. The results are presented in Fig. 2(a) as bar charts (abbreviations and identifiers of the solvents can be found in SI, Section 4). We remind the reader that the lower the  $\ln \gamma_{\text{PCA-5mer}}^\infty$  value, the higher the PCA-5mer/solvent thermodynamic affinity; therefore, the solvent efficiency increases from right to left in Fig. 2(a). Although some highly dipolar, toxic solvents, such as NMP and DMSO, are predicted by COSMO-SAC to exhibit better affinity with PCA-5mer than GVL, GVL is among the most effective solvents and ranks second among green alternatives, following DMI. Interestingly, GVL is predicted to be more efficient than the toxic and dipolar acetonitrile. The predicted negative  $\ln \gamma_{\text{PCA-5mer}}^\infty$  value in GVL indicates negative deviations from ideal mixture behavior, which is a favorable factor in terms of the dissolution and solubility of PCA-5mer or lignin.

Next, the COSMO-SAC analysis was extended to water/solvent binary mixtures. Fig. 2(b) shows the predicted course of  $\ln \gamma_{\text{PCA-5mer}}^\infty$  as a function of water mole percent in aqueous mixtures of five selected solvents: DMI, GVL, THF, 1,4-dioxane, and BHGBL. Interestingly, in each considered system,  $\ln \gamma_{\text{PCA-5mer}}^\infty$  does not follow a simple, monotonic trend between its

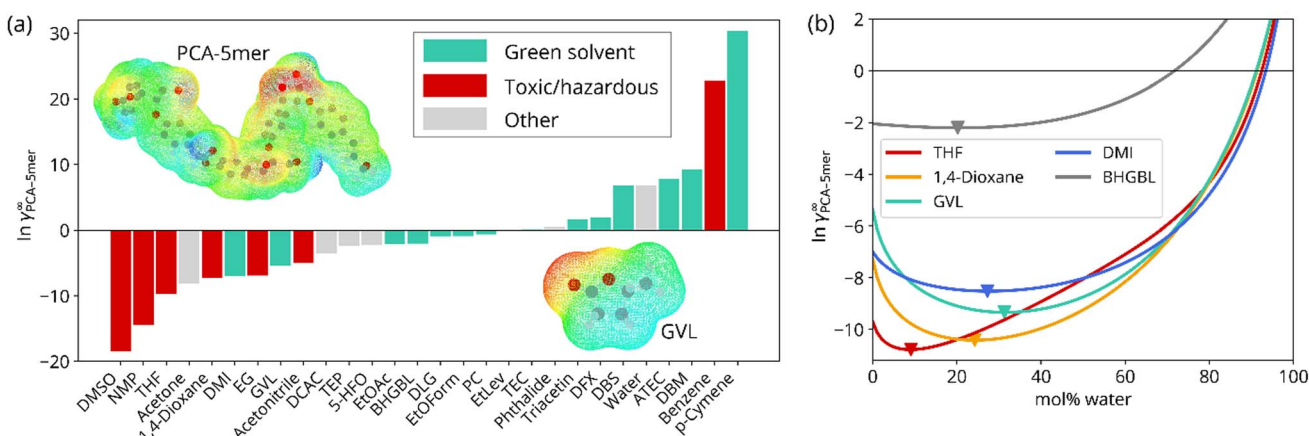


Fig. 2 Activity coefficients of PCA-5mer at infinite dilution in (a) various neat solvents and (b) five selected water/solvent binary mixtures as a function of water mol%, as predicted by the open-source COSMO-SAC model. All results correspond to a temperature of 298 K. Solvent abbreviations are provided in SI Section S4. (a) also includes electrostatic potential maps of the solute PCA-5mer and solvent GVL, calculated using QM at the DFT/BVP86/TZVP/C-PCM level as part of their  $\sigma$ -profile determination. The triangles in (b) indicate the minima on the respective curves.



values in the pure organic solvent and pure water but instead exhibits a (favorable) minimum. This suggests that adding water (from small amounts up to 30–70 mol% water, depending on the specific solvent/water system) enhances the solvent efficiency for PCA-5mer, compared to the neat solvent, despite water itself having very poor affinity for hydrophobic PCA-5mer, as shown in Fig. 2(a). This indicates a strong cooperative effect between the considered solvents and water and highlights the importance of excess thermodynamic properties in the case of non-additive solution behavior. The only exception where the cooperative effect is not as significant is the aqueous solution of BHGBL. This can be explained by the fact that, while the other four organic solvents exhibit only hydrogen bond acceptor ability, BHGBL contains a hydroxyl group, making it both a hydrogen bond donor and acceptor. This dual character may increase the “similarity” between water and BHGBL, rendering their mixture more thermodynamically ideal and thus lacking a significant extremum in  $\ln \gamma_{\text{PCA-5mer}}^{\infty}$ .

The position and “depth” of the  $\ln \gamma_{\text{PCA-5mer}}^{\infty}$  minimum, corresponding to maximum solubility enhancement, vary between systems. For GVL/water, the minimum was predicted to occur at 70 mol% GVL, which corresponds to 93 wt% GVL. This fully supports the 9/1 (wt/wt) GVL/water ratio used in experiments in this and previous research<sup>39</sup> and aligns perfectly with the optimal GVL weight percent (92–96%) estimated by Lé *et al.*<sup>51</sup> using Hildebrand solubility parameters. Another interesting observation concerns the two green solvents: DMI and GVL. While pure DMI was predicted to be slightly more efficient than pure GVL (see Fig. 2(a)), mixing with water reverses their relative order. The decrease in  $\gamma_{\text{PCA-5mer}}^{\infty}$  values is more pronounced for the GVL/water system, resulting in a lower minimum  $\gamma_{\text{PCA-5mer}}^{\infty}$  than that observed for DMI/water, as shown in Fig. 2(b).

The observations made in this section align with experimental findings of lignin solubility in GVL/water mixtures at different compositions. GVL/water mixtures dissolved default organosolv lignin in different amounts, leading to the ternary

phase diagram depicted in SI Section S5. In contrast to recent findings from Lé *et al.*,<sup>101</sup> who predicted the highest solubility of lignin to be in pure GVL, our solvent mixture of GVL/water showed a clear increase in lignin solubility at mixtures of GVL with low weight percentages of water. The lignin solubility was 45 wt% in a GVL/water 9/1 wt/wt mixture, and 40 wt% in pure GVL. The full ternary phase diagram can be seen in SI Section S5. These experimental findings correlate with the simulation findings and also add to the suggestion of a synergistic effect of water and GVL at high GVL weight percentages. At low GVL percentages, lignin begins to show only minimal solubility, which is used when precipitating the extracted lignin from the extraction solvent *via* the addition of large amounts of water.

The predictive thermodynamic analysis performed in this section with COSMO-SAC also identified the GVL/water system with *ca.* 9/1 (wt/wt) ratio as an optimal solvent medium candidate for lignin, balancing efficiency with sustainability. However, COSMO-SAC provides only limited insight into the behavior of systems at the molecular and atomic levels. Therefore, the following section presents the results of MD simulations conducted to elucidate finer interactional and structural aspects of the GVL/water system with PCA-5mer as the solute.

**3.1.2 MD simulations.** In order to rationalize the microscopic origin of lignin, atomistic MD simulations of PCA-5mer in neat solvents and in the equimolar GVL/water mixture were performed. For a detailed insight into PCA-5mer/solvent interactions, spatial distribution functions were used to visualize locations of significantly increased density of solvent molecules (opaque clouds indicate regions with 5× higher-than-average density, while transparent clouds indicate 3×). The distributions of water oxygen, carbonyl oxygen of GVL (representing the polar part) and ring carbon of GVL (representing the non-polar part) around the PCA-5mer molecule are presented in Fig. 3. These results demonstrate that pure water (left panel, red clouds) interacts primarily with the polar hydroxyl (OH) groups of PCA-5mer, to much lesser extent affinity with the faces of aromatic ring, but the non-polar part of

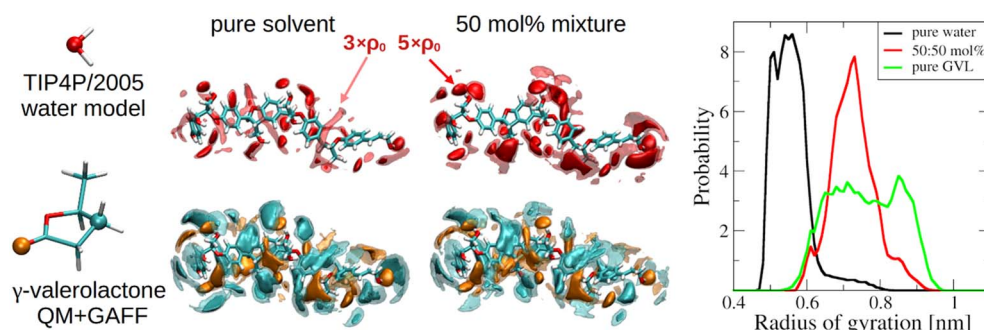


**Fig. 3** Synergy in hydration and solvation of a swollen configuration ( $R_g \sim 0.85$  nm) of PCA-5mer in pure solvents (left) and in their 50 mol% (ca. 85 w%) mixture (right). Spatial distribution of water (oxygen in red), polar carbonyl oxygen of GVL (in gold), and non-polar carbon atom of GVL (in cyan) are shown at two isocontour levels: 3x and 5x increased probabilities are denoted as transparent and opaque clouds (as illustrated by red arrows on water oxygen distributions). Compared to pure solvents, both water hydration of hydroxyl groups and hydrophobic interaction of GVL with hydrophobic moieties are significantly strengthened, with mild decrease of GVL carbonyl H-bonding interaction with hydroxyl groups. Impact of solvent quality (water vs. GVL) on a PCA-5mer conformation is captured in distribution of polymer size (radius of gyration), in the most right panel. Visualization of the regions of increased density of solvent molecules, analysis for collapsed configuration of PCA-5mer and comparison of solvation of rigid structures to flexible ensembles are provided in detail in the SI Section S6.

**Table 1** Analysis of the lignin content for different types of biomasses, including wood and different waste streams, using the CASA method described in chapter 2.7.2. The lignin was extracted through the GVL-assisted organosolv process described in chapter 2.2. The extractions were conducted in triplicates, meaning each biomass sample was used as a substrate three subsequent times to remove most of the lignin from the biomass. The yield is given as a percentage of the determined lignin content in the respective type of biomass. Additionally, the purity of the extracted lignin was determined through the CASA method, as certain extractives (degraded sugars, proteins, ash) might be co-extracted and reside in the lignin samples

Type of biomass	Lignin content [wt%]	Step 1 extraction yield [% of lignin content]	Step 1 lignin purity [%]	Step 2 extraction yield [% of lignin content]	Step 2 lignin purity [%]	Step 3 extraction yield [% of lignin content]	Step 3 lignin purity [%]	Tripletate extraction yield [% of lignin content]	Purity of extracted lignin [%]
Spruce sawdust	22 ± 1	57 ± 2	94 ± 1	28 ± 1	93 ± 1	12 ± 1	93 ± 1	97 ± 3	93 ± 1
Coffee silverskin	21 ± 1	61 ± 2	96 ± 1	21 ± 2	96 ± 1	5 ± 1	96 ± 1	87 ± 6	96 ± 1
Walnut shell	28 ± 1	53 ± 1	94 ± 1	27 ± 1	93 ± 1	10 ± 0	93 ± 1	90 ± 2	93 ± 1
Hazelnut shell	29 ± 1	51 ± 1	95 ± 1	28 ± 0	93 ± 1	13 ± 0	93 ± 1	92 ± 1	93 ± 1
Peanut skin	26 ± 1	46 ± 1	94 ± 1	34 ± 0	90 ± 1	15 ± 0	90 ± 1	95 ± 1	90 ± 1
Peanut shell	33 ± 1	41 ± 1	87 ± 1	34 ± 0	83 ± 1	14 ± 1	83 ± 2	89 ± 2	83 ± 2
Pistachio shell	15 ± 1	43 ± 1	91 ± 1	33 ± 1	89 ± 3	14 ± 0	89 ± 3	90 ± 2	89 ± 3
Almond shell	29 ± 1	50 ± 2	91 ± 1	30 ± 1	90 ± 1	12 ± 0	90 ± 1	92 ± 3	90 ± 1
Cashew shell	27 ± 1	45 ± 4	95 ± 2	32 ± 1	93 ± 3	15 ± 1	96 ± 4	92 ± 6	96 ± 4
Beech sawdust	22 ± 1	51 ± 1	94 ± 1	28 ± 1	94 ± 1	15 ± 0	93 ± 1	94 ± 2	93 ± 1
Birch sawdust	23 ± 1	53 ± 1	94 ± 1	27 ± 0	94 ± 1	15 ± 0	93 ± 1	95 ± 1	93 ± 1

PCA-5mer remains poorly hydrated. In contrast, the overall attractive GVL-PCA-5mer interactions arise favorable interaction between carbonyl oxygen of GVL (gold clouds) with polar OH groups combined with favorable interactions between the non-polar moieties of GVL (cyan clouds) and the aromatic ring and attached aliphatic group of PCA-5mer. The amphiphilic nature of GVL thus rationalizes its efficiency in the lignin dissolution since both polar and non-polar parts of PCA-5mer are well solvated in GVL.

Since both experimental results and COSMO-SAC analysis indicate that the *ca.* 9/1 (wt/wt) GVL/water mixture is optimal for efficient PCA-5mer/lignin dissolution, we decided to investigate the intermolecular interactions occurring in the equimolar mixture of GVL and water. Note that equimolar composition of GVL/water mixture corresponds to approximately 85 wt% GVL which is close to the optimal mixture composition used in the experimental part of this paper. The analysis of the equimolar GVL/water mixture reveals that interactions of carbonyl oxygens of GVL with OH groups of PCA-5mer are partially replaced by stronger hydrogen bonds with water. This enhanced selective hydration of PCA-5mer hydroxyls is complemented by the stabilizing interaction between non-polar domain of PCA-5mer and non-polar part of GVL molecule, as water only poorly hydrates the hydrophobic regions of PCA-5mer. These concerted interactions between water, GVL and the PCA-5mer surface are visually documented in Fig. 3, where growing clouds indicate regions of increased solvent density. These structural changes are quantified in SI Section S6. Major changes occur within the first solvation shell (~4 Å) around the polar and non-polar regions of PCA-5mer. There is a shift towards better PCA-5mer solvation when transitioning from pure solvent to the equimolar mixture. Therefore, the presence of GVL in the solvent mixture allows water to selectively interact with the polar parts of PCA-5mer, while the non-polar part of GVL provides stabilizing interactions with the aromatic ring of PCA-5mer. This synergistic effect results in a more efficient solubilization of PCA-5mer compared to pure solvents. This effect is conditioned by the complete miscibility of GVL and water.

These results suggest that the intermolecular interactions occurring in the GVL/water mixture with PCA are not merely a trivial combination of effects occurring in pure solvents. This insight opens a new pathway for future theoretical studies focused on aqueous mixtures of GVL (or similar solvents) with the aim to systematically and more thoroughly examine the nature of these interactions and their impact on biomass component dissolution. More importantly, these insights also support the effectiveness of the GVL/water mixture, and herein the green solvent GVL, in lignocellulosic biomass fractionation, as the solvent can effectively dissolve and thus separate lignin from biomass.

### 3.2 GVL-assisted biomass fractionation

**3.2.1 Lignin extraction using acidic GVL/water mixtures.** In this main part of the study, the focus was on experimentally determining whether the chosen extraction process, which is



based on knowledge gained by our theoretical considerations, could extract lignin and hemicellulose in high yields and purities from various biomass sources with the green solvent GVL, leaving behind a lignin-free natural cellulosic fiber. Multiple biomass sources were examined for lignin extraction and qualitative analysis, aiming for an efficient process of lignin separation. The results for lignin content, yield, and purity for all the different biomass sources studied are summarized in Table 1. These data are crucial for evaluating the potential for each biomass feedstock for further valorization possibilities and for refining the extraction process to maximize the efficiency of lignin recovery and purity. By comparing the lignin yields and purities from different biomasses for the two extraction processes, conclusions can be drawn on how to efficiently extract lignin from lignocellulosic biomass without wasting the potential of the residual biopolymers.

The lignin isolated from biomass through the default GVL-based extraction process was qualitatively identified through <sup>1</sup>H-NMR spectroscopy to confirm the extraction products.

The different biomass sources showed very different overall lignin contents, which is due to their different structural properties. Woods like beech, birch and spruce show lignin contents from 22–23 wt%. Generally, nutshells show a higher lignin content (27–33 wt%), which can be attributed to their overall more rigid structure with higher mechanical strength

and reduced water absorptivity, making them more durable and protected.<sup>102</sup> Nutshells also have specialized cells called sclereids, that are heavily lignified, contributing to the overall higher lignin content and to the hardness of the shell.<sup>103</sup> These cells only occur in the part of the biomass that is the shell, meaning that typical nut skins show lower lignin contents, which can be seen in the lignin contents of coffee silverskin and peanut skin (21–26 wt%).

Overall, all biomasses enabled high triplicate lignin extraction yields from 89–97% with high purity values from 83–96% depending on the biomass source. GVL/water (9/1 wt/wt) proved to be an effective solvent for lignin extraction for not only wood residues but also different lignocellulosic waste streams like nutshells or nut skins. This underlines the biodiversity of using the process based on GVL for lignocellulosic biomass extraction. The efficiency of the process was still improvable, as high yields of lignin were only achieved after three subsequent extraction steps at high temperatures of 120 °C. The extraction yield decreased with higher extraction steps, as less lignin is present in the fiber structure. Residual lignin also showed higher condensation when examining the fractions through 2D-HSQC-NMR spectroscopy, which could be seen in an increasingly overlapping signal for the aromatic subunits G and S for lignin fractions from higher extraction steps (Fig. 4(b)). The condensation mechanism of lignin structures is shown in

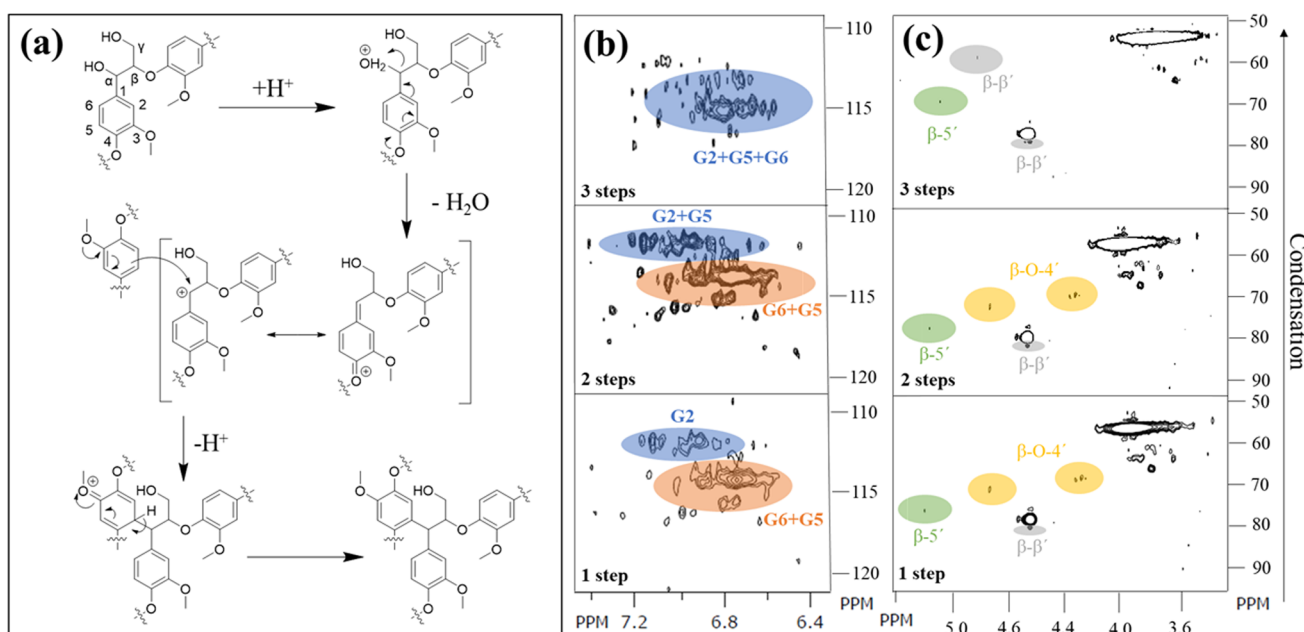


Fig. 4 (a) Lignin condensation process, starting from a guaiacol subunit with β-1,4-diol function and ether linkage to another guaiacol subunit, representing the guaiacol-rich hardwood lignin of spruce sawdust. The condensation reaction is an acid-catalyzed nucleophilic aromatic substitution, with another lignin fragment forming a C–C bond with the starting lignin molecule. The product, condensed lignin, can further undergo condensation, forming a highly complex and random lignin structure.<sup>76,77</sup> (b) 2D-HSQC-NMR spectrum excerpts of extracted lignin from spruce sawdust biomass after different numbers of extraction steps (1, 2, and 3 extraction steps). The excerpts show the aromatic region of the 2D-HSQC-NMR spectra, ranging from 6.4 to 7.3 ppm on the <sup>1</sup>H-scale (x-axis), and from 110 to 120 ppm on the <sup>13</sup>C-scale (y-axis), respectively. Due to its hardwood nature, spruce sawdust lignin consists mainly of guaiacol subunits. The signals for G2, G5, and G6 are labelled inside the spectra. An overlap of multiple guaiacol subunit signals in the 2D-HSQC-NMR indicates condensation of lignin structures. (c) 2D-HSQC-NMR spectrum excerpts of the aliphatic region after a different number of extraction steps. Labelled green are β-5' linkages, labelled grey are β-β' linkages, and labelled yellow are β-O-4' linkages. The disappearance of ether linkage signals indicates increasing condensation with more extraction steps.



Fig. 4(a). The first extraction steps yielded 41–61% lignin, second extraction steps yielded 21–34% lignin, and third extraction steps yielded 5–15% lignin, depending on the biomass origin. The purity of the lignin from different extraction steps did not show any significant changes, which is probably due to no change in extraction conditions. Another reason for the decrease in lignin extraction efficiency with the number of extraction steps is the increase in condensation of lignin structures. This is shown in Fig. 4(b). Lignin, extracted from the guaiacyl (G) rich hardwood biomass spruce, already shows medium condensation after the first extraction step, which is indicated by the H/C chemical shifts in the HSQC-NMR excerpts. Signals for G5 (usually at 6.48–7.06/115.0–120.5 ppm) and G6 (usually at 6.65–6.96/120.5–124.5 ppm) overlap and form a uniform signal at 6.53–7.12/114.5–117.5 ppm, indicating condensation. With an increasing number of extraction steps, the overlap of G signals increases. At extraction step 2, the G5+G6 signal (now 6.55–7.14/112.3–115.2 ppm) shifts more towards the G2 (6.71–7.19/110.8–112.9 ppm) signal, starting to overlap. After extraction step 3, the extracted lignin shows large condensation, as G2, G5, and G6 signals all overlap in a uniform signal at 6.60–7.01/113.1–115.9 ppm. The condensation is also shown in the aliphatic region of the HSQC-NMR spectra. With more extraction steps, the already low intensity  $\beta$ -O-4' signals at 4.36/69.1 ppm and 4.64/71.2 ppm disappear, leaving only the signals for carbon–carbon linkages of  $\beta$ -5' (5.21/70.2 ppm) and  $\beta$ - $\beta'$  (4.54/82.7 ppm) linkages, with a new signal for  $\beta$ - $\beta'$  rising from the background at 4.63/58.9 ppm after extraction step 3. For the exact experimental assignment of the signals, see SI Section S3. The resulting condensed lignin structures become more complex and less consistent. With the decrease in hydroxy groups and the increase in C–C bonds, the lignin structures become more thermally and chemically stable. This also comes with a loss in polarity and an increase in structural rigidity,<sup>104</sup> making its solvent penetration and solubilization with the intermediately polar solvent GVL more challenging.

For the extraction process, GVL is essential due to its ability to dissolve the lignin very efficiently. GVL acts as the main solvent for the fractionation of all biopolymers in lignocellulosic biomass, creating a green solvent mixture for the process. Due to its size and intermediate polar properties, GVL cannot only swell the biopolymer structure, but then disrupt hydrogen bonding and hydrophobic interactions between cellulose and lignin-hemicellulose-complexes. This leads to lignin being isolated from the main cellulose fiber much easier than with other green solvents.<sup>105–107</sup> Additionally, acidic conditions are necessary to break apart the large lignin structures into smaller oligomers, enabling their dissolution in the solvent system. Many applications can be considered for isolated lignin from various waste streams, depending on its composition.

Condensed lignin structures might form stronger interactions with the cellulose and hemicellulose components in the biomass, coming from increased hydrophobic interactions between the now more hydrophobic lignin and hydrophobic parts of the other biopolymers,<sup>108</sup> and the reduced flexibility of the lignin structures.<sup>109</sup> Another reason for this can be the increased hydrogen bonding strength between lignin hydroxy

groups, now surrounded by larger high electron density aromatic systems,<sup>110</sup> and cellulose/hemicellulose hydroxy groups. Additionally,  $\pi$ – $\pi$  stacking interactions between large aromatic domains of lignin molecules might increase, which also adds to the decreased extraction efficiency.<sup>104</sup> To efficiently extract lignin with GVL from biomass, the extraction method had to be altered to preserve native lignin structures (these only include native C–C linkages). This should increase the extraction efficiency by preserving an intermediately polar lignin structure, while creating lignin extraction products with consistent structural properties. This will be addressed in the following chapter.

Before any lignin extraction, some biomasses can provide valuable extractives that can be separated from the fiber part of the biomass before. These extractives are low molecular weight compounds extrinsic to the plant cell walls to protect them from degradation and growth alteration agents like bacteria or fungi. They can be divided into terpenoids, polyphenols, waxes and fats, salts of organic acids, proteins, and alkaloids. The exact extractive composition depends largely on the type and nature variance of a certain lignocellulosic biomass.<sup>111</sup> The simple removal of valuable extractives before insoluble fiber fractionation was conducted for coffee silverskin, which is very rich in caffeine and certain polyphenols. These were extracted with water in a multicycle process, which was studied in a separate work with Chemat *et al.* (2024).<sup>112</sup> By removing these extractives, the CASA lignin content and the purity did not change, which verifies the insignificance of partly aromatic extractives in the employed lignin purity determination method. This concludes that by a simple cascade process, different extractives can be separated from certain biomasses with green solvents before fractionation of the insoluble fibers, creating more valuable products. This can be very interesting in terms of valorization of waste-biomass, like coffee silverskin or other waste products.

**3.2.2 Aldehyde-assisted lignin extraction.** For the modified lignin and hemicellulose extraction process from lignocellulosic biomass, the method of aldehyde-assisted fractionation, first established by Lan *et al.* (2018),<sup>41</sup> was adapted and optimized for our process based on GVL. This method uses aldehydes as protecting agents for the  $\beta$ -1,4-diol functions in lignin polymers, forming acetal-functionalities in the process. While this process does not use GVL/water mixtures from the start, the aqueous solution of HCl provides enough water to establish the synergistic solvent effect that was found with the COSMO-SAC and MD simulations. The reaction of the acetal-protection process is depicted in Fig. 5(a). These acetals cannot be broken down in the lightly acidic environment of extraction, thus protecting the lignin structures from condensation during the extraction process. This was expected to yield more consistent lignin structures with higher ether-contents and an overall more consistent structure. These lignin structures were also expected to be more suitable for subsequent hydrogenolysis towards lignin monomers, as higher overall ether-contents and less condensed aromatic structures lead to more cleavable sites between lignin subunits. This process was previously conducted with 1,4-dioxane but was now performed with GVL under mild conditions. The optimization of extraction parameters has



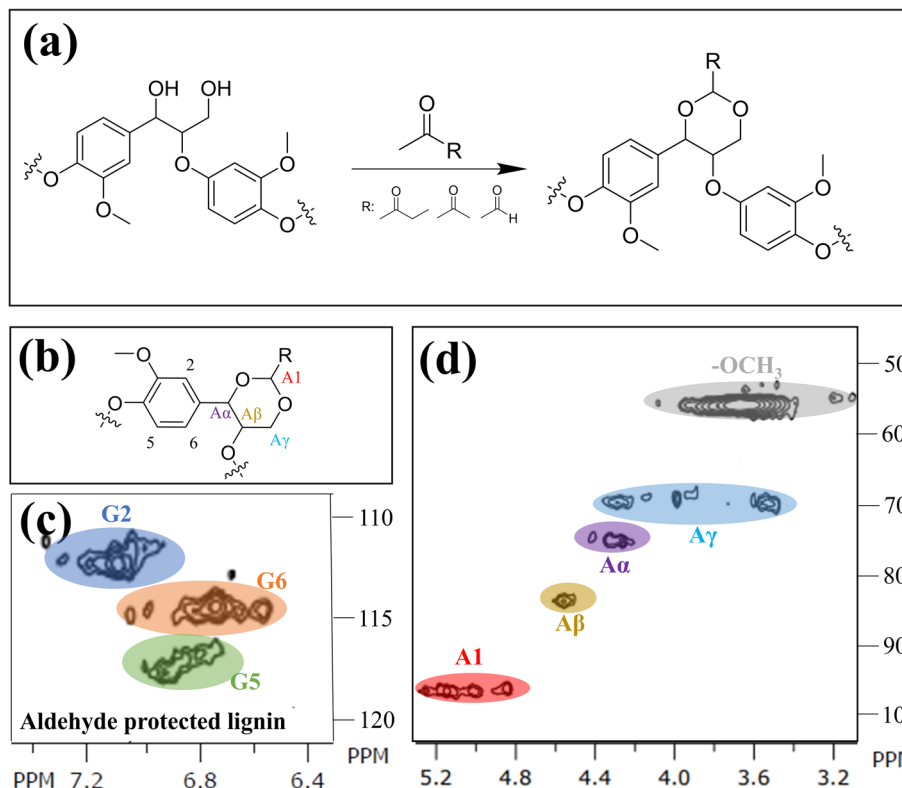


**Fig. 5** (a) Aldehyde induced protection reaction of  $\beta$ -1,4-diol functions in lignin structures. The reaction takes place in a lightly acidic environment within the solvent GVL. For this work, propionic aldehyde, acetaldehyde, and formaldehyde were used. Full acetals are formed, protecting lignin structures from condensation. (b) Nomenclature of protected lignin structures after aldehyde protection reaction for this work. (c) 2D-HSQC-NMR spectrum excerpt from spruce sawdust lignin after aldehyde-assisted extraction. For the guaiacol-rich spruce lignin, the signals in the aromatic region for G2, G5, and G6 are distinctly visible in the excerpt. The x-axis shows the  $^1\text{H}$ -scale, and the y-axis shows the  $^{13}\text{C}$ -scale for the 2D-HSQC-NMR spectrum excerpt. Distinctly visible signals for each aromatic proton linked to its carbon instead of signal overlap show the successful prevention of lignin condensation. Instead, the structure of native lignin was preserved during the extraction. (d) 2D-HSQC-NMR spectrum excerpt from spruce sawdust lignin after aldehyde-assisted extraction. The excerpt shows the aliphatic region from 3.2–5.2 ppm on the  $^1\text{H}$ -x-axis and 50–100 ppm on the  $^{13}\text{C}$ -y-axis. The signals for the acetal-protected lignin linkage structures A1, A $\alpha$ , A $\beta$ , and A $\gamma$ , as well as signals for methoxy groups, and residual native  $\beta$ - $\beta'$  and  $\beta$ - $5'$  linkages are assigned respectively. The intensity of native C–C linkage signals and thus their compositional percentage depends entirely on the source of biomass used for lignin extraction.

shown that 13% solid loading of dried and ground biomass, 84/16 wt/wt of GVL/aldehyde (in this case, propionic aldehyde was used) mixture composition, and  $0.34 \text{ mol L}^{-1}$  of hydrochloric acid at a temperature of  $85^\circ\text{C}$  for an extraction time of 3 h were the optimal extraction conditions (more details for process optimization see SI, Section S2). The lignin yield (calculated through comparison with the theoretical yield in eqn (1) due to alteration of molecular weight of lignin after acetal functionalization) and purity for each biomass using this improved method, as well as the lignin protection rate analyzed through 2D-HSQC-NMR (details see SI Section S3) is shown in Table 2.

Overall, the modified process achieves higher lignin yields with higher purities after only one extraction step than the default extraction process achieves after triplicate extraction steps on the same biomass. In contrast to the dioxane-based aldehyde assisted extraction process, the partly mentioned advantages of the GVL-based aldehyde assisted extraction process are manifold: zero solvent toxicity, no solvent flammability, no formation of explosive hydroperoxides, solvent recovery without degradation, green synthesis, or

biodegradability. However, all these advantages are only relevant if the performance of the GVL process is comparable. The optimized process conditions (with non-polar precipitation) were used with both solvents to obtain a performance comparison of both methods. Spruce and birch were used as the extracted biomass. Both isolated lignins behaved and appeared very similar, with highly similar yields, and both sharing zero extraction-based condensation. In summary, GVL offers a highly similar performance as a solvent in biomass fractionation compared to dioxane. Differences in the quality of the isolated lignins are not significant. These are highly promising results for the future use of GVL as the solvent in AAF biorefineries or for developing new biomass fractionation procedures. The protection of the  $\beta$ -1,4-diol groups was very successful, leading to protection rates of 100% for lignin from every examined biomass source. The 2D-HSQC-NMR signals for the protection group hydrogen atoms are shown in Fig. 5(d), and the signals for the lignin subunit compositions are shown in Fig. 5(c) (both for spruce sawdust lignin).



**Table 2** Lignin quantitative analysis for the modified extraction process using an acidic mixture of GVL/propionic-aldehyde, including the overall lignin content for each biomass determined through CASA UV/vis spectroscopy, the extraction yield calculated through eqn (1), the purity of extracted lignin determined through CASA UV/vis spectroscopy, and the lignin protection rate analyzed through 2D-HSQC-NMR spectroscopy

Type of biomass	Lignin content [wt%]	Extraction yield [% of lignin content]	Purity of extracted lignin [%]	Lignin protection rate [%]
Spruce sawdust	22 ± 1	99 ± 1	99 ± 1	100 ± 0
Coffee silverskin	21 ± 1	96 ± 2	97 ± 1	100 ± 0
Walnut shell	28 ± 1	95 ± 2	96 ± 1	100 ± 0
Hazelnut shell	29 ± 1	95 ± 1	96 ± 1	100 ± 0
Peanut skin	26 ± 1	95 ± 1	97 ± 1	100 ± 0
Peanut shell	33 ± 1	93 ± 2	93 ± 2	100 ± 0
Pistachio shell	15 ± 1	92 ± 2	94 ± 2	100 ± 0
Almond shell	29 ± 1	95 ± 3	97 ± 1	100 ± 0
Cashew shell	27 ± 1	93 ± 6	97 ± 1	100 ± 0
Beech sawdust	22 ± 1	99 ± 1	98 ± 1	100 ± 0
Birch sawdust	23 ± 1	97 ± 1	99 ± 1	100 ± 0

The  $\beta$ -1,4-diol structures were converted to acetal groups, which can be examined through the signal assignment for the respective A1 (4.72–5.28/98.3–99.5 ppm), A $\alpha$  (4.10–4.39/74.5–77.9 ppm), A $\beta$  (4.37–4.60/83.2–86.4 ppm), and A $\gamma$  (3.37–4.38/68.7–72.0 ppm) signals. These signals are assigned in the aliphatic region of the spectrum in Fig. 5(d). The disappearance of ether linkage signals usually at 4.36/69.1 ppm and 4.64/71.2 ppm, and of the signals for carbon–carbon linkages of  $\beta$ -5' (5.21/70.2 ppm) and  $\beta$ - $\beta'$  (4.54/82.7 ppm) into the background, allows the interpretation that due to the protection of lignin structures with aldehydes, no ether linkage is unprotected and no condensation occurred during extraction. Signals for native  $\beta$ -O-4' linkages were not retained. The  $\beta$ -O-4' linkages were quantitatively replaced by acetal functions, with some  $\beta$ -O-4' linkages also being broken down during extraction. Thus, the lignin received after aldehyde-assisted extraction from biomass retained its native structure besides cleavage at random ether linkages due to the acidic environment. The extraction-based condensation is effectively zero, which is underlined by signals for G2 (6.97–7.30/111.0–113.8 ppm), G5 (6.76–7.03/116.1–118.9 ppm), and G6 (6.54–7.07/114.1–115.9 ppm) being distinctly visible and showing no overlap. Using only one extraction step with largely milder conditions, compared to the default extraction process, preserves a large part of the lignin structure while interrupting intermolecular interactions to separate lignin from the carbohydrate fibers and eventually dissolve it in the GVL-based solvent. Comparing the extraction of lignin from spruce sawdust with aldehyde protecting agents at 85 °C (yield: 99%) to the extraction without aldehyde protecting agents (default extraction process) at 85 °C (yield: 5%), both after one extraction step, there is a clear gap in extraction yield. Reducing extraction-based condensation to effectively zero, the lignin can be extracted in its native form under milder conditions. Also, precipitation-based condensation was eliminated by switching the precipitation system from water towards a *n*-heptane/ethyl acetate based system. Using water led to lower protection and higher condensation even with the aldehyde extraction process (for more details, see SI Section S2). With the protection of the diol groups, the polarity of the lignin is only

slightly decreased compared to unprotected lignin. Instead of condensed, largely hydrophobic lignin, the now extracted lignin structures stay intermediately polar,<sup>113</sup> retaining the ability to be readily dissolved by GVL at high percentages. For condensed lignin, hydroxy groups at the  $\gamma$ -position can form stronger hydrogen bonds with cellulose and hemicellulose due to the increased electron density through the enlarged aromatic surrounding.<sup>110</sup> When using the aldehyde-protection process, lignin hydroxy groups are fully converted to acetals. This completely prevents hydrogen bonding between lignin  $\beta$ -O-4' linkage domains and cellulose/hemicellulose fibers, enabling an efficient separation and subsequent dissolution in GVL. Still, hydrogen bonding can occur due to the presence of *e.g.* free phenolic hydroxy groups or ether linkages in the lignin structure. The swelling process of the biomass also plays a big role in efficient dissolution of lignin. Due to the flexibility and intermediate polarity of the acetal-protected lignin structures, solvent molecules have a much easier way of migrating into the biopolymer structure, swelling it and enabling dissolution by interrupting intermolecular hydrophobic interactions and hydrogen bonding interactions between lignin and cellulose/hemicellulose. The residual native C–C linkages that are present in lignin structures after extraction are only of small concentrations in most woods (beech, birch, spruce). Carbon linkages are more prevalent in lignin of more rigid biomasses, as they provide rigidity and less flexibility to the lignin and thus to the overall fiber structure. A correlation can be seen in the achieved lignin yields for different biomasses after aldehyde-assisted extraction. Lignin from biomasses such as nutshells achieve slightly lower yields compared to woods. In lignin from these biomasses, the content of native C–C linkages is also higher than in lignin from woods.<sup>114</sup> This native condensation of aromatic units provides stability and rigidity, but also slightly decreases the potential for efficient extraction of lignin. This again confirms the correlation between condensation and extraction efficiency for this GVL-based extraction process.

In summary, the aldehyde-assisted GVL-based lignin extraction process leads to effectively no condensation between lignin structures during extraction, which leads to almost



complete lignin removal after one extraction step at milder conditions than with the default extraction process. This is influenced by the different properties of the acetal-protected lignin compared to the condensed lignin. Native lignin condensation only slightly influences the extraction efficiency, but greatly influences the rigidity of the biomass source.

**3.2.3 Hemicellulose extraction.** After the extraction of lignin and separation through either heptane or aqueous precipitation, the hemicellulose residues dissolved in the liquid fraction can be recovered through reduced pressure evaporation of the solvent. For the default extraction process using an acidic mixture of GVL/water, the hemicellulose residues are a mixture of monomeric sugars like xylose and glucose, which can be separated and further processed towards sugar-based products (see upcoming article). For the modified extraction process using an acidic mixture of GVL/protecting agent, these monomeric sugars are obtained in their acetal protected form. These acetal-protected sugar molecules show great perspectives for valorization, as the protection groups can be varied and even modified to yield different functionalities attached to the sugar molecules. Their qualitative assessment through 2D-HSQC-NMR spectroscopy and their structures, extracted from beech wood sawdust, are shown in Fig. 6.

Since beech wood has a xyloglucan backbone and thus a high xylose and glucose content, the yield (see Table 3, for all biomasses) of hemicellulose decomposition products and their composition (45 mol% of protected xylose, 40 mol% of protected glucose, 15 mol% of different other protected hexoses or pentoses, determined through quantitative  $^1\text{H}$ -NMR, see SI Section S3) were determined. Using the GVL/protecting agent

modified extraction process, monomeric protected sugars can be extracted in high yields and purities from all types of biomasses. The purity here describes the presence of lignin or cellulose residues in the hemicellulose solution, which is 0% for all biomass sources due to the insolubility of lignin and cellulose in the hemicellulose solvent. Since lignin fully precipitates in the precipitation medium, and cellulose fully precipitates in the extraction solvent, the hemicellulose residue was completely lignin- and cellulose-free. From the default extraction process, lignin-hemicellulose complexes are more intact during and after extraction, making it more difficult to separate

**Table 3** Hemicellulose content for different biomass sources determined in through the carbohydrate determination method. The hemicellulose yields for the default extraction process and the aldehyde-assisted extraction process are given in respect to the overall hemicellulose content

Type of biomass	Hemicellulose content [wt%]	Hemicellulose yield default [%]	Hemicellulose yield prot. [%]
Spruce sawdust	25 $\pm$ 3	80 $\pm$ 4	98 $\pm$ 1
Coffee silverskin	32 $\pm$ 3	82 $\pm$ 3	91 $\pm$ 1
Walnut shell	22 $\pm$ 1	81 $\pm$ 6	96 $\pm$ 3
Hazelnut shell	22 $\pm$ 1	81 $\pm$ 4	95 $\pm$ 3
Peanut skin	19 $\pm$ 2	75 $\pm$ 2	93 $\pm$ 1
Peanut shell	16 $\pm$ 2	77 $\pm$ 2	93 $\pm$ 1
Pistachio shell	22 $\pm$ 2	81 $\pm$ 4	96 $\pm$ 1
Almond shell	23 $\pm$ 1	84 $\pm$ 6	95 $\pm$ 4
Cashew shell	11 $\pm$ 1	68 $\pm$ 3	86 $\pm$ 1
Beech sawdust	31 $\pm$ 1	87 $\pm$ 1	97 $\pm$ 1
Birch sawdust	32 $\pm$ 1	85 $\pm$ 2	97 $\pm$ 1

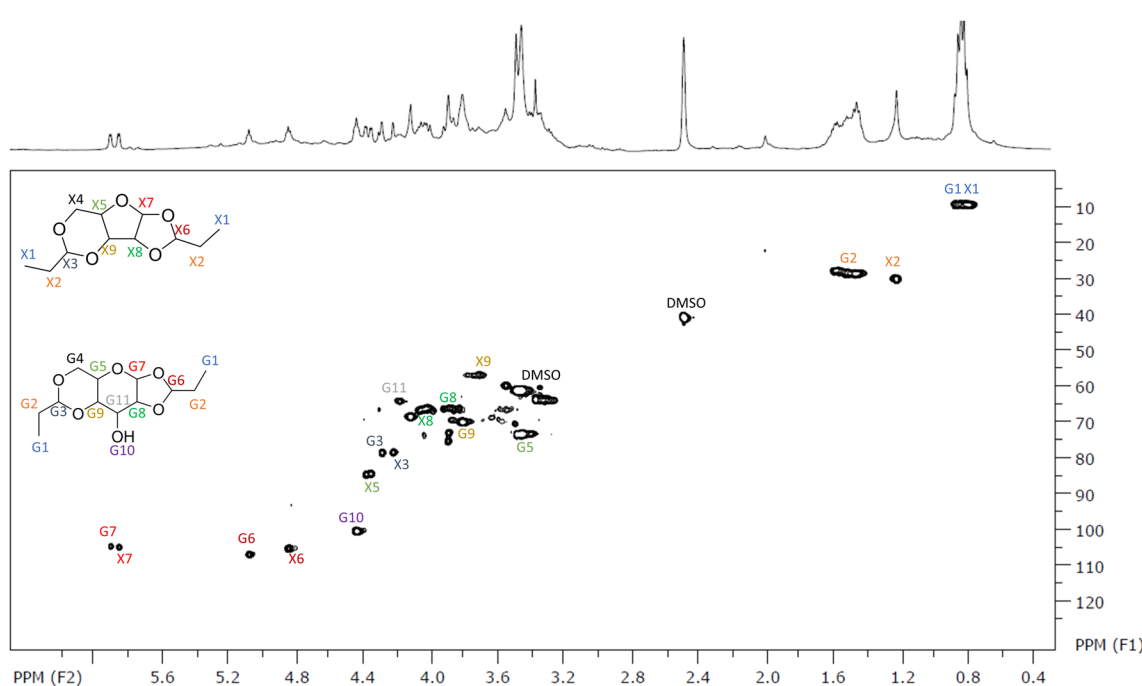


**Fig. 6** 2D-HSQC-NMR spectrum of the residual hemicellulose fraction from beech wood sawdust. Hemicellulose was decomposed into protected sugar units; in this case the protection agent was propionic aldehyde. Protected xylose and glucose are depicted in the spectrum with their respective signal assignments to specific protons and carbon atoms.



hemicellulose from the other biopolymers. This leads to lower purities for both cellulose and lignin in the default extraction process due to hemicellulose residues present in their structure. The aldehyde-assisted extraction process in a GVL-based medium provides higher one-step yields of hemicellulose residues at milder conditions, which however now are di-acetalized. These protected sugar monomers can be tuned and used for various applications in the future. Their possible valorization will be addressed over the next articles.

**3.2.4 Cellulose fractionation.** From the improved lignin and hemicellulose extraction process using an acidic mixture of GVL/water/protecting agent at 85 °C, cellulose was recovered through simple filtration, washing and mild drying processes. To analyze the yield and purity of cellulose from each extracted biomass sample, the cellulose content was determined using simple acid hydrolysis, and the cellulose purity after lignin and hemicellulose extraction was determined using the CASA method, of which the results are shown in Table 4.

An important note is that the lignin-free cellulose was received after one single lignin/hemicellulose extraction step with the aldehyde-assisted GVL extraction process (~0.6 wt% residual lignin for spruce sawdust measured with CASA), compared to the default extraction process using only an acidic mixture of GVL/water at 120 °C, which led to less pure cellulose (~3.2 wt% residual lignin for spruce sawdust measured with CASA) even after 3 subsequent extraction steps. To dissolve the cellulose, it is important to first completely remove the lignin and hemicellulose, as it interacts with the cellulose chains, forming lignin-hemicellulose-complexes around the chains and acting as a sort of fiber-glue, preventing efficient dissolution.<sup>115</sup> The aldehyde-assisted GVL extraction process removes more lignin and hemicellulose from the cellulose chains under milder conditions and less extraction steps (92–99%) compared to the default extraction process (87–97%). This also leads to cellulose being less degraded due to a lower possibility of polysaccharide hydrolysis. Additionally, only very small amounts of natively condensed lignin structures stick with the cellulose chains leading to higher cellulose purity for the aldehyde-assisted process (>99%) compared to the default

process (>89%). This enables the cellulose from the aldehyde-assisted extraction process for further valorization. One particular way of cellulose valorization is connected to its efficient dissolution and regeneration to produce fibers. Current processes are either not green or not efficient enough,<sup>116</sup> which is why the problem of dissolving cellulose in a biodiverse dissolution process will be addressed in future work.

### 3.3 Overview of the process for complete green lignocellulosic biomass dissolution

The overarching goal of this research was to complete a process for the full and biodiverse fractionation of all components of lignocellulosic biomass using green solvent mixtures at mild conditions. GVL in an acidic mixture of GVL/water/lignin-protecting-agent at 85 °C proved to be effective in separating lignin and hemicellulose in an uncondensed way from lignocellulosic biomass, leaving behind pure cellulose. Hemicellulose is degraded to sugar units, mostly xylose and glucose, during the extraction process. The protecting agent that is responsible for extracting uncondensed lignin structures also protects the sugar molecules over acetal functions, leading to stable protected sugar molecules that can be isolated. Fig. 7 shows a simple visualization for the full process studied in this work, including all process products.

The lignin extraction was compared between an acidic GVL/water mixture and an acidic GVL/water/aldehyde mixture. Using aldehydes to protect the  $\beta$ -1,4-diol groups in lignin structures from condensation can be efficiently done in GVL to achieve full protection. This leads to higher lignin yields, higher lignin purity, and effectively no extraction-based condensation. The condensation of lignin structures influences their polarity, flexibility, and thus their solubilization and swelling behavior for specific solvents. Using aldehydes as protecting agents provides native lignin structures without altered properties, that can be deprotected and further broken down towards valuable monomers, which will be addressed in future work. The protected monomeric sugar units were also received from the extraction process and analyzed qualitatively and quantitatively. Using different biomasses leads to different yields of

**Table 4** Cellulose content determined through acid hydrolysis for every biomass. The cellulose yield (determined gravimetrically) and purity (determined through CASA method) after a default extraction using an acidic mixture of GVL/water are given. Additionally, the cellulose yield and purity after the modified extraction using an acidic mixture of GVL/protecting agent are given

Type of biomass	Cellulose content [%]	Cellulose yield default [%]	Cellulose purity default [%]	Cellulose yield prot. [%]	Cellulose purity prot. [%]
Spruce sawdust	43 ± 1	91 ± 2	97 ± 1	97 ± 2	99 ± 1
Coffee silverskin	22 ± 3	87 ± 5	93 ± 1	98 ± 1	99 ± 1
Walnut shell	40 ± 1	92 ± 3	95 ± 3	97 ± 2	99 ± 1
Hazelnut shell	41 ± 1	92 ± 1	96 ± 2	97 ± 2	99 ± 1
Peanut skin	35 ± 2	90 ± 4	94 ± 1	98 ± 2	99 ± 1
Peanut shell	41 ± 2	90 ± 3	94 ± 1	98 ± 2	99 ± 1
Pistachio shell	56 ± 2	89 ± 3	92 ± 3	96 ± 1	99 ± 1
Almond shell	39 ± 1	93 ± 1	96 ± 2	97 ± 1	99 ± 1
Cashew shell	37 ± 4	81 ± 5	89 ± 7	93 ± 4	99 ± 1
Beech sawdust	41 ± 1	92 ± 3	97 ± 1	98 ± 2	99 ± 1
Birch sawdust	40 ± 1	93 ± 2	96 ± 2	98 ± 1	99 ± 1



## Wood dissolution process using GVL

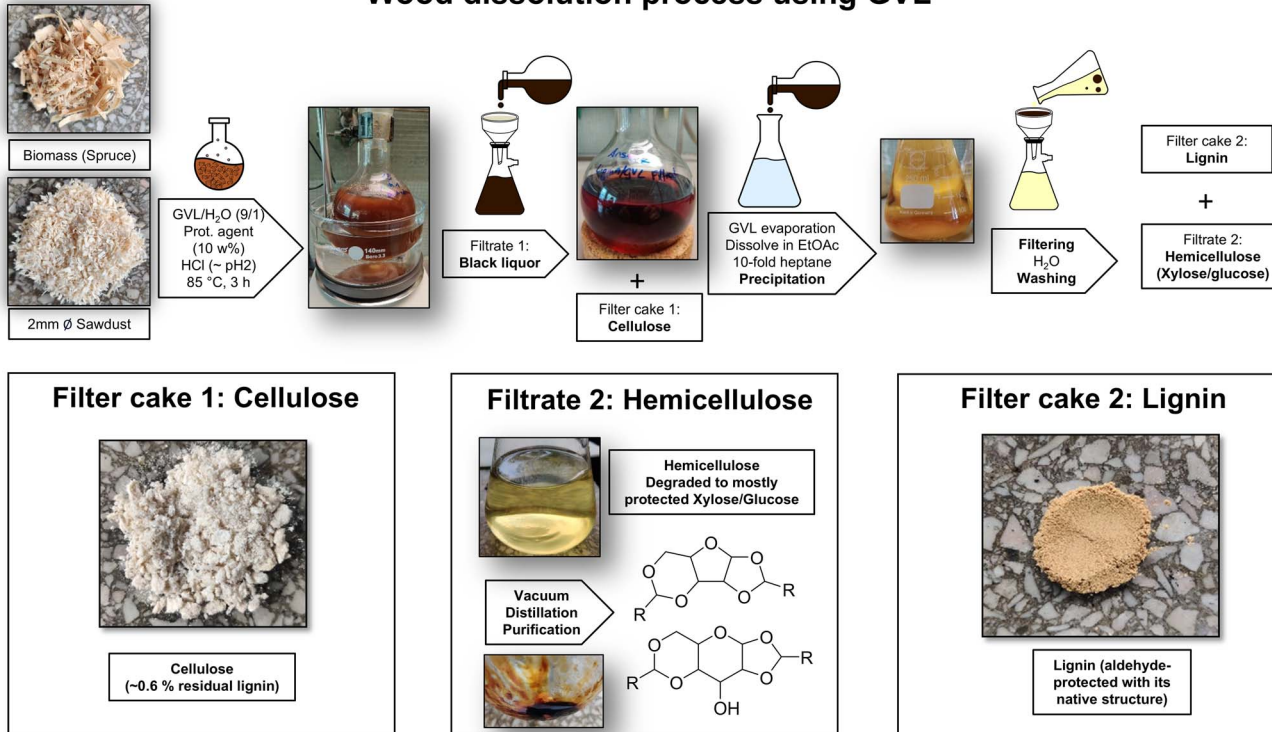


Fig. 7 Visualization of the complete lignocellulosic biomass separation, dissolution, and degradation using the green solvent GVL. Zero waste is left from the initial biomass. This process can be used for every lignocellulosic biomass, be it wood, nutshells, or different lignocellulosic waste-streams.

xylose, glucose, and smaller amounts of different hexoses and pentoses, as hemicellulose composition varies depending on the origin biomass. Depending on the need for certain applications, other protected sugars can be isolated for biomasses that have a low xylose content and higher contents of other sugar monomers. For protected xylose and glucose, applications can be found by varying the protecting agent and performing modification reactions, introducing functional groups into the xylose/glucose structure that can, *e.g.*, induce curing reactions in resin formulations. Additionally, xylose can always be deprotected in a slightly acidic environment and used to produce the solvent GVL.<sup>117</sup> The isolated cellulose was analyzed on its yield and purity, which was compared for a default extraction process using only an acidic mixture of GVL/water, and a modified extraction process introducing a protecting agent for lignin and hemicellulose extraction. The latter yielded a purer cellulose after one extraction step at milder conditions compared to three extraction steps at harsher conditions for the default extraction process. The purer cellulose can be used for further valorization, which involves finding a green and efficient solvent for cellulose dissolution. Lowering the dissolution temperature and increasing the soluble amount of cellulose while maintaining the fast dissolution times and low viscosities are all challenges on cellulose solubilization that will be addressed in future work. The detailed, stepwise overview of the

fractionation and decomposition of lignocellulosic biomass is finally shown in Fig. 8.

Our process of complete biomass fractionation tackles different problems of many other solvent systems that have been developed for this purpose. Most organosolv processes use highly flammable or hazardous solvent mixtures in large amounts, resulting in high costs for emissions and solvent consumption.<sup>56,68–70</sup> The problem of using hazardous solvents and having high solvent production costs is also a problem of processes based on IL's, including their difficult recovery.<sup>57,58,60</sup> Using acidic mixtures of GVL/aldehyde with small amounts of water significantly lowers the solvent consumption of the extraction to a minimum of 1 mL solvent per 0.15 g of biomass in our process. The solvent consumption of the lignin separation through precipitation could be more than halved by using a nonpolar precipitation route. Moreover, GVL and water, forming 97% of the solvent mixture, are considered green solvents due to low vapor pressure, low flammability, and general non-toxicity. However, the aldehyde used can pose minimal risks, as some aldehydes we used are classified as hazardous (propionic aldehyde, acetaldehyde). These could and should be used stoichiometrically and be replaced with less hazardous alternatives, like benzaldehyde. Also, the washing step and the precipitation system include solvents like heptane, ethyl acetate, methanol, and diethyl ether, which should all be replaced by greener alternatives in the future. For now, their use



# Lignocellulose fractionation using GVL-AAF

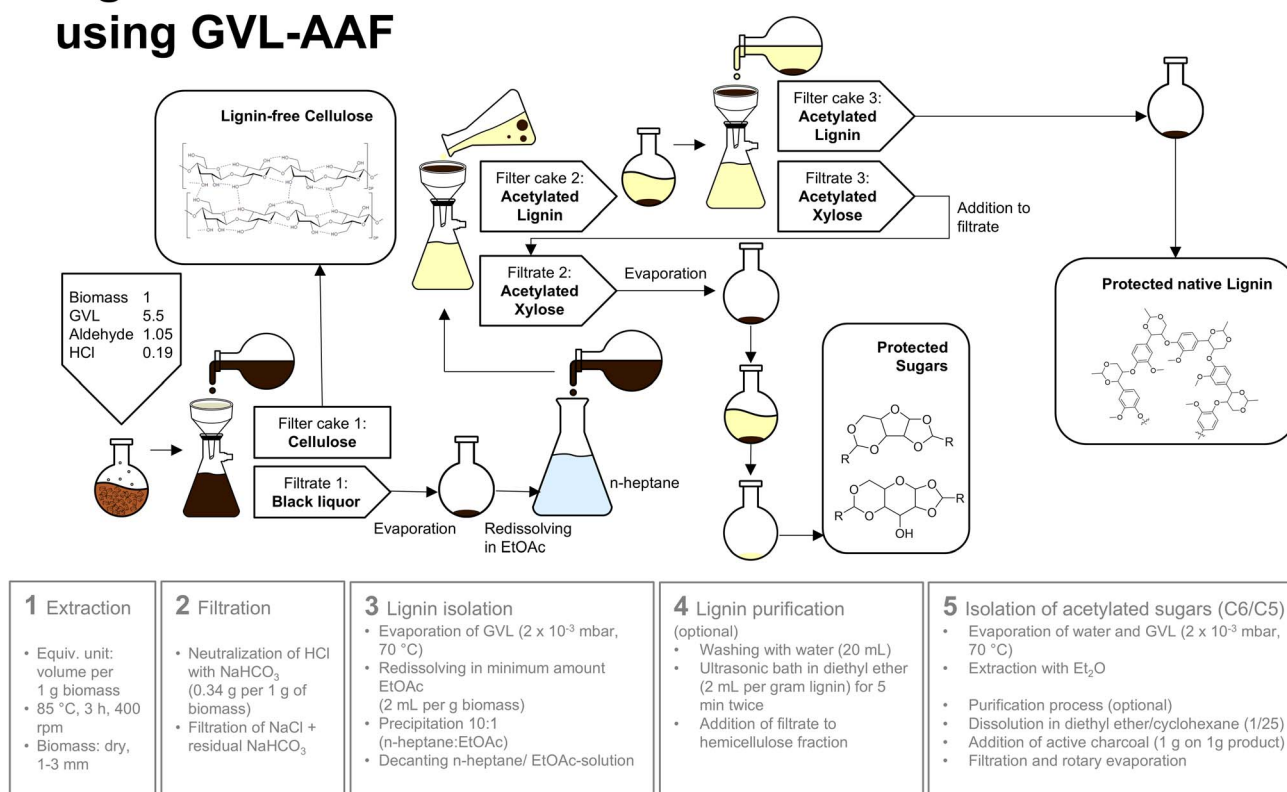


Fig. 8 Detailed overview of the fractionation of lignocellulosic biomass and conversion towards monomeric lignin and hemicellulose units.

reduces the solvent consumption for precipitation and the efficiency of the lignin workup. The solvent mixture itself is also fully reusable and achieves similar results after a reuse in the extraction process. After separation of the biopolymers, pure GVL, water, and residual aldehyde could be regained through simple evaporation. With the regeneration of the original composition, the solvent mixture can be fully reused. To increase solvent availability, GVL can even be produced from hemicellulose fractionation products.<sup>117</sup> To further reduce energy consumption of the recycling process, ways have to be found to separate the solvents from the biopolymers through liquid–liquid extraction or similar methods.

A bigger problem in suggested biomass fractionation processes, including organosolvents, DES, and IL's, is the high process energy consumption,<sup>57,58,64,65</sup> coupled to a medium efficiency with not necessarily all biopolymers being accessible in high quality.<sup>59,62,63,66,67</sup> While some processes achieve complete fractionation with high yields, their product quality is not sufficient enough for every biopolymer, and their process energy consumption is very high, usually using temperatures of  $>160$  °C, long reaction times  $>24$  h and high pressures.<sup>56</sup> Our process combines a comparably mild method, only using 85 °C and 3 h of full processing time under slightly acidic conditions (pH  $\sim$ 2). Still, our process can fractionate all biopolymers in very high yields with very high purities. Additionally, the quality of the biopolymers is not altered significantly from their

appearance in lignocellulosic biomass. Lignin structures are broken down into large oligomers, preserving their native structure through acetal-protection, which can be lifted in acidic medium. Many other pulping processes alter the structure of the lignin or introduce condensation, which blocks certain ways of valorization.<sup>23–29</sup> Hemicellulose is regained in monomeric form as mainly protected xylose and protected glucose, leaving room for different valorization options. Cellulose is regained lignin-free and can be used for different processes like the production of cellulosic fibers or enzymatic hydrolysis towards sugars. Possible improvements to our process could of course include the further reduction of process energy consumption, retaining the achieved quality of the fractionated biopolymers. Another huge advantage of our process is its biodiversity. While other processes specifically mention their use on one specific type of biomass,<sup>59,62,63</sup> our process has been adapted to serve the fractionation of many different types of biomasses. This includes typical woods, but also more or less waste streams like nutshells or coffee silver-skin. Also, the only pretreatment is their drying to remove extensive moisture contents. However, a future challenge will be the scalability of this process, as this process will have to be integrated with existing biorefinery infrastructure, especially the further use of extracted biopolymer products.

Lignin can be used in many applications, such as antioxidant formulations,<sup>33,34,118</sup> UV-protection films or coatings for food or

human skin,<sup>30-32</sup> as flocculants after chemical modification,<sup>119</sup> or in bio-based phenolic resins.<sup>120,121</sup> Specifically, lignin monomers can be produced, which can have further valuable applications. This includes uses as flavor or fragrance ingredients, as monolignols like 4-propyl-syringol or 4-propyl-guaiacol are already considered as such.<sup>35,122,123</sup> They can also be regarded as antioxidants.<sup>124</sup> A very important application can be the use of lignin and hemicellulose monomers in various bio-based resin formulations. This topic is currently researched by our group and will be regarded in the future in a separate publication. Lignin monomers can therefore act as bisphenol A substitutes in epoxy resins, as curing agents after chemical modification, or as monomeric units in other resin types. A similar application can be found for degraded hemicellulose products, specifically protected xylose and glucose molecules. By varying the protecting agent, different functional groups can be introduced that can induce an application as resin monomers. To round out the process of green dissolution of lignocellulosic biomass, xylose, specifically after deprotection in lightly acidic medium, can always be used to produce GVL for further extractions.<sup>46-48</sup> Both biopolymers show valuable applications after considering their molecular structure after extraction and selecting the optimal biomass for a certain application.

While cellulose was regained lignin-free and must be dissolved for further use. The dissolution of cellulose is a big problem nowadays, as existing processes are neither green enough (they use too much energy or produce hazardous by-products) nor efficient enough. Process alternatives or improvements have to be found in order to dissolve and regenerate cellulose fibers to produce many valuable bio-based products.<sup>125-130</sup> This topic will be addressed in the future in an upcoming project.

What separates our process from existing literature on GVL-based organosolv processes is the overall yield of uncondensed lignin. While existing literature finds mostly up to 60% of lignin yield at typical organosolv conditions,<sup>39</sup> which is then very condensed and prohibits a further use in several applications or degradation processes, and disregards other biopolymers present in biomass, our process combines the GVL organosolv process with the aldehyde-assisted process, yielding then up to 99% uncondensed lignin after a single extraction step under milder conditions. Additionally, the biopolymers cellulose and hemicellulose can be retained in very high purity up to 99%. This shows that our process can be the next step in realizing GVL-based biorefinery, producing all components of lignocellulosic biomass in high yields and purities with green solvents and mild conditions. An important note is that our process uses biodiverse starting material, from lignocellulosic waste materials such as nutshells to different types of wood, with no clear setback in process efficiency.

While this article describes the basis of a scalable process for sustainable biomass fractionation, follow-up articles will describe the detailed extraction and characterization of lignin with different properties depending on the extraction conditions, making a tailoring of lignin products for specific applications possible.<sup>131</sup> Additionally, we will follow-up on the cellulose fractionation by introducing novel cellulose

dissolution strategies involving our lignin-free cellulose from biomass. Regarding the hemicellulose degradation products, we are currently working on the valorization options for the protected sugars in resin formulations or solvent applications, which will also be addressed in future works.

## 4 Conclusion and outlook

GVL, especially in combination with water at 9/1 wt/wt, can dissolve lignin in an effective way to facilitate biomass fractionation. This was underlined through the use of COSMO-SAC and MD simulations, which showed that the presence of GVL in the solvent allows water to interact with polar parts of lignin more efficiently, while GVL itself interacts with the aromatic core of lignin structures in a stabilizing manner. This makes for a synergistic effect between GVL and small amounts of water compared to the pure solvents. Thorough systematic computational investigations of dissolution capabilities of pure and mixed solvents on biomass components by means of both COSMO-SAC and MD simulations will be conducted as separate studies.

Experimentally, starting from source-independent lignocellulosic biomass, the theoretical considerations on the simplified lignin system were proven to be right as it was shown that the green solvent GVL can efficiently fractionate all its main fiber components, lignin, hemicellulose, and cellulose. The process of using GVL with lignin protection-agents greatly improves biopolymer fractionation, leading to native lignin structures with high yields and purities, acetylated hemicellulose monomers, and lignin-free cellulose. The process uses mild conditions of 85 °C and 3 h reaction time, while also providing complete reusability of the solvents. This completes a full biodiverse fractionation process of lignocellulosic biomass, improving on existing processes in literature and leading to three valuable and pure biopolymer products that can be further studied for their valorization. This work will be continued in our future research on lignin and hemicellulose valorization, tailoring their properties during extraction for specific applications, and on cellulose dissolution for industrial fiber production using novel approaches to replace existing processes.

Overall, this work provides clear insights into the green, mild, and biodiverse fractionation of lignocellulosic biomass with GVL and its possible ways of improvement and further valorization of the high quality biopolymer products. Our process of biomass fractionation combines significant advantages of previously developed processes, while improving on their problems. Still, improvements to parts of the process, such as solvent consumption or replacement of the protection agents with greener alternatives have to be made to achieve full implementation of this process in biorefinery.

## Author contributions

Moritz Schweiger: conceptualization, data curation, investigation, formal analysis, visualization, methodology, writing – original draft. Thomas Lang: investigation, formal analysis,



validation. Eva Müller: writing – review & editing, supervision, conceptualization. Didier Touraud: conceptualization, writing – review & editing. Werner Kunz: writing – review & editing, supervision, resources, project administration, funding acquisition. Vojtěch Jeřábek: investigation, formal analysis, visualization, writing – original draft. Martin Klajmon: investigation, formal analysis, data curation, visualization, writing-original draft, methodology, funding acquisition. Jan Heyda: investigation, formal analysis, data curation, visualization, writing – original draft. Magdalena Bendová: writing – review & editing, resources. Karel Řehák: writing – review & editing, resources.

## Conflicts of interest

There are no conflicts to declare.

## Data availability

Should any data files be needed in another format, they are available from the corresponding author upon reasonable request.

The data supporting this article have been included in the text and as part of the SI. See DOI: <https://doi.org/10.1039/d5su00600g>.

## Acknowledgements

The German authors acknowledge the financial support of KVT-Technology (Graz, Austria) and their cooperation with our department of physical chemistry II at the University of Regensburg. We also acknowledge the support of the project “AI-supported search for environmentally acceptable solvents for the dissolution and stabilization of biopolymers for their utilization as sustainable materials”, funded by the Bayerisch-Tschechische Hochschulagentur (BTHA) as project BTHA-JC-2024-57. The Czech authors acknowledge the financial support from the LUABA24070 joint project of The Ministry of Education, Youth and Sports of the Czech Republic and The Bavarian-Czech Academic Agency. This work was also supported by the project “The Energy Conversion and Storage”, funded as project No. CZ.02.01.01/00/22\_008/0004617 by Programme Johannes Amos Comenius, call Excellent Research and by the Ministry of Education, Youth and Sports of the Czech Republic through the e-INFRA CZ (ID:90254). V. J. acknowledges the support of the grants of Specific university research – grants No. A1\_FCHI\_2025\_001 and No. A2\_FCHI\_2025\_009.

## References

- 1 A. Lorenz, When will we run out of fossil fuels?. *Fairplanet: Sustainable Consumption*; 2023, cited 2024 Jan 20, available from, <https://www.fairplanet.org/story/when-will-we-run-out-of-fossil-fuels/>.
- 2 F. Kähler, O. Porc and M. Carus, *RCI Carbon Flows Report: Compilation of Supply and Demand of Fossil and Renewable Carbon on a Global and European Level*, Nova Institute, 2023.
- 3 C. Ververis, K. Georghiou, N. Christodoulakis, P. Santas and R. Santas, Fiber dimensions, lignin and cellulose content of various plant materials and their suitability for paper production, *Ind. Crops Prod.*, 2004, **19**(3), 245–254.
- 4 B. O. Abo, M. Gao, Y. Wang, C. Wu, H. Ma and Q. Wang, Lignocellulosic biomass for bioethanol: an overview on pretreatment, hydrolysis and fermentation processes, *Rev. Environ. Health*, 2019, **34**(1), 57–68.
- 5 B. Singh, J. Korstad, A. Guldhe and R. Kothari, Editorial: Emerging Feedstocks & Clean Technologies for Lignocellulosic Biofuel, *Front. Energy Res.*, 2022, **10**, 917081.
- 6 M. Mujtaba, L. F. Fraceto, M. Fazeli, S. Mukherjee, S. M. Savassa, G. A. de Medeiros, *et al.*, Lignocellulosic biomass from agricultural waste to the circular economy: a review with focus on biofuels, biocomposites and bioplastics, *J. Cleaner Prod.*, 2023, **402**, 136815.
- 7 E. Kocaturk, T. Salan, O. Ozcelik, M. H. Alma and Z. Cancan, Recent Advances in lignin-Based Biofuel Production, *Energies*, 2023, **16**(8), 3382.
- 8 V. Ashokkumar, K. Ramaswamy, M. Popat, M. Asokan, S. Devendran, K. Arutselvan, *et al.*, Recent advances in lignocellulosic biomass for biofuels and value-added bioproducts – a critical review, *Bioresour. Technol.*, 2022, **344B**, 126195.
- 9 H. Li, S. Saravanamurugan, A. Pandev and S. Elumalai, Biochemicals and materials production: an introduction, in *Biomass, Biofuels, Biochemicals: Biochemicals and Materials Production from Sustainable Biomass Resources*, Elsevier Inc., 2022, pp. 1–8.
- 10 B. Xu, J. Dai, Z. Du, F. Li, H. Liu, X. Gu, *et al.*, Catalytic conversion of biomass-derived compounds to various amino acids: status and perspectives, *Front. Chem. Sci. Eng.*, 2023, **17**, 817–829.
- 11 A. Jaswal, P. P. Sing and T. Mondal, Furfural – a versatile, biomass-derived platform chemical for the production of renewable chemicals, *Green Chem.*, 2022, **24**(2), 510–551.
- 12 P. A. Son, S. Nishimura and K. Ebitani, Production of  $\gamma$ -valerolactone from biomass-derived compounds using formic acid as a hydrogen source over supported metal catalysts in water solvent, *RSC Adv.*, 2014, **4**(21), 10525–10530.
- 13 N. Singh, R. R. Singhania, P. S. Nigam, C. Dong, A. K. Patel and M. Puri, Global status of lignocellulosic biorefinery: Challenges and perspectives, *Bioresour. Technol.*, 2022, **344B**, 126415.
- 14 X. Zhou, L. J. Broadbelt and R. Vinu, Mechanistic Understanding of Thermochemical Conversion of Polymers and Lignocellulosic Biomass, *Adv. Chem. Eng.*, 2016, **49**, 95–198.
- 15 E. Jamet, H. Canut, G. Boudart and R. F. Pont-Lezica, Cell wall proteins: a new insight through proteomics, *Trends Plant Sci.*, 2006, **11**(1), 0–39.
- 16 J. Berglund, K. Svedström, M. Khayyami and P. Gatenholm, Wood hemicelluloses exert distinct biomechanical contributions to cellulose fibrillar networks, *Nat. Commun.*, 2020, **11**, 4692.



17 H. V. Scheller and P. Ulvskov, Hemicelluloses, *Annu. Rev. Plant Biol.*, 2010, **61**, 263–289.

18 R. W. Dstroy, M. E. Himmel, J. O. Baker, W. S. Adney, S. R. Thomas, R. A. Nieves, *et al.*, Bioconversion of wheat straw cellulose/hemicellulose to ethanol by *Saccharomyces uvarum* and *Pachysolen tannophilus*, *Biotechnol. Bioeng.*, 1982, **24**(5), 1105–1113.

19 P. H. F. Pereira, W. R. Waldman, J. M. Marconcini and L. H. C. Mattoso, Wheat straw hemicellulose added with cellulose nanocrystals and citric acid: Effect on film physical properties, *Carbohydr. Polym.*, 2017, **164**, 317–324.

20 X. Liu, J. Ren, J. Song, X. Fu, S. Wang, Y. Zhou, *et al.*, Hemicellulose from plant biomass in medical and pharmaceutical application: A critical review, *Curr. Med. Chem.*, 2019, **26**(14), 2430–2455.

21 P. Nechita, R. Mirela and F. Ciolacu, Xylan Hemicellulose: a renewable material with potential properties for food packaging applications, *Sustainability*, 2021, **13**(24), 13504.

22 P. Kalita, P. Datta and P. K. Baruah, Conversion of fructose and xylose into platform chemicals using organo-functionalized mesoporous material, *ChemistrySelect*, 2018, **3**, 10971–10976.

23 M. Graglia, *Lignin Valorization [PhD Thesis]*, University of Potsdam, 2017.

24 C. Chio, M. Sain and W. Qin, Lignin utilization: a review of lignin depolymerization from various aspects, *Renewable Sustainable Energy Rev.*, 2019, **107**, 232–249.

25 S. H. Ghaffar and M. Fan, Lignin in straw and its applications as an adhesive, *Int. J. Adhes. Adhes.*, 2014, **48**, 92–101.

26 R. M. Trevorah and M. Z. Othman, Alkali Pretreatment and Enzymatic Hydrolysis of Australian Timber Mill Sawdust for Biofuel Production, *J. Renewable Energy*, 2015, **2015**, 284250.

27 D. S. Bajwa, G. Pourhashem, A. H. Ullah and S. G. Bajwa, A concise review of current lignin production, applications, products and their environmental impact, *Ind. Crops Prod.*, 2019, **139**, 111526.

28 S. Jampa, A. Puente-Urbina, Z. Ma, S. Wongkasemjit, J. S. Luterbacher and J. A. van Bokhoven, Optimization of Lignin Extraction from Pine Wood for Fast Pyrolysis by Using a  $\gamma$ -Valerolactone-Based Binary Solvent System, *ACS Sustain. Chem. Eng.*, 2019, **7**(4), 4058–4068.

29 D. Watkins, M. Nuruddin, M. Hosur, A. Tcherbi-Narteh and S. Jeelani, Extraction and characterization of lignin from different biomass resources, *J. Mater. Res. Technol.*, 2015, **4**(1), 26–32.

30 G. K. K. Anushikha, Lignin as a UV blocking, antioxidant, and antimicrobial agent for food packaging applications, *Biomass Convers. Biorefin.*, 2023, **14**, 16755–16767.

31 A. Halloub, M. Raji, H. Essabir, H. Chackchak, R. Boussen, M. Bensalah, *et al.*, Intelligent food packaging film containing lignin and cellulose nanocrystals for shelf life extension of food, *Carbohydr. Polym.*, 2022, **296**, 119972.

32 M. H. Tran, D. Phan and E. Y. Lee, Review on lignin modifications toward natural UV protection ingredient for lignin-based sunscreens, *Green Chem.*, 2021, **23**(13), 4633–4646.

33 X. Lu, X. Gu and Y. Shi, A review on lignin antioxidants: their sources, isolations, antioxidant activities and various applications, *Int. J. Biol. Macromol.*, 2022, **210**, 716–741.

34 S. Kang, J. Chang and J. Fan, Phenolic Antioxidant Production by Hydrothermal Liquefaction of Lignin. Energy Sources A: Recovery Util, *Environ. Eff.*, 2015, **37**(5), 494–500.

35 T. Ren, Z. Zhang, S. You, W. Qi, R. Su and Z. He, Isolation and purification of 4-propylguaiacol and 4-propylsyringol by extraction and crystallization from the products of reductive catalytic fractionation processes, *Green Chem.*, 2022, **24**(19), 7355–7361.

36 Y. Li, J. Zhu, Z. Zhang and Y. Qu, Preparation of Syringaldehyde from Lignin by Catalytic Oxidation of Perovskite-Type Oxides, *ACS Omega*, 2020, **5**(5), 2107–2113.

37 M. Fache, B. Boutevin and S. Caillol, Vanillin Production from Lignin and its Use as a Renewable Chemical, *ACS Sustain. Chem. Eng.*, 2016, **4**(1), 35–46.

38 C. Isola, H. L. Sieverding, A. M. Numan-Al-Mobin, R. Rajappagowda, E. A. Boakye, D. E. Raynie, *et al.*, Vanillin derived from lignin liquefaction: a sustainability evaluation, *Int. J. Life Cycle Assess.*, 2018, **23**, 1761–1772.

39 F. Cheng, S. Liu, S. D. Karlen, H. Kim, F. Lu, J. Ralph, *et al.*, Poplar lignin structural changes during extraction in  $\gamma$ -valerolactone (GVL), *Green Chem.*, 2023, **25**(1), 336–347.

40 C. Gioia, M. Colonna, A. Tagami, L. Medina, O. Sevastyanova, L. A. Berglund, *et al.*, Lignin-Based Epoxy Resins: Unravelling the Relationship between Structure and Material Properties, *Biomacromolecules*, 2020, **21**(5), 1920–1928.

41 W. Lan, M. T. Amiri, C. M. Hunston and J. S. Luterbacher, Protection Group Effects During  $\alpha,\gamma$ -Diol Lignin Stabilization Promote High-Selectivity Monomer Production, *Angew. Chem., Int. Ed.*, 2018, **57**(5), 1356–1360.

42 J. H. Clark and J. Duncan, *Handbook of Green Chemistry and Technology*, Blackwell Science Ltd, 2002.

43 P. T. Anastas and J. C. Warner, *Green Chemistry: Theory and Practice*, Oxford University Press, 1998, p. 30.

44 C. Y. Y. Wong, A. W. Choi, M. Y. Lui, B. Fridrich, A. K. Horváth, L. T. Mika, *et al.*, Stability of gamma-valerolactone under neutral, acidic, and basic conditions, *Struct. Chem.*, 2017, **28**, 423–429.

45 C. Ortiz-Cervantes, M. Flores-Alamo and J. J. Garcia, Hydrogenation of biomass-derived levulinic acid into  $\gamma$ -valerolactone catalyzed by palladium complexes, *ACS Catal.*, 2015, **5**(3), 1424–1431.

46 B. Liu, X. Chen, Y. Xu, C. Qiao, Z. Lu and Y. Tian, A combo Zr-zeolite and Zr(OH)<sub>4</sub> mixture composition for one-pot production of  $\gamma$ -valerolactone from furfural, *Renewable Energy*, 2024, **229**, 120751.

47 B. Qiu, J. Shi, W. Hu, Y. Wang, D. Zhang and H. Chu, Efficient and selective conversion of xylose to furfural over carbon-based solid acid catalyst in water- $\gamma$ -valerolactone, *Energy*, 2024, **294**, 130774.



48 J. Qiu, Y. Liu, J. Zhang, B. Zhou, Q. Yang, L. Zhang, *et al.*, One-pot cascade process for efficient upgrading of furfural to  $\gamma$ -valerolactone over adjustable Lewis-Bronsted bi-acidic catalyst, *Ind. Crops Prod.*, 2024, **214**, 118474.

49 D. di Menno di Buccianico, G. E. Scarponi, J.-C. Buvat, S. Levener and V. C. Moreno, From biomass-derived fructose to  $\gamma$ -valerolactone: process design and techno-economic assessment, *Bioresour. Technol.*, 2024, **401**, 130753.

50 J. S. Luterbacher, J. M. Rand, D. M. Alonso, J. Han, J. T. Youngquist, C. T. Maravelias, *et al.*, Nonenzymatic sugar production from biomass using biomass-derived  $\gamma$ -valerolactone, *Science*, 2014, **343**(6168), 277–280.

51 H. Q. Le, A. Zaitseva, J.-P. Pokki, M. Stahl, V. Alopaeus and H. Sixta, Solubility of organosolv lignin in  $\gamma$ -valerolactone/water binary mixtures, *ChemSusChem*, 2016, **9**, 2939–2947.

52 B. Yang, S. Zhang, H. Hu, C. Duan, Z. He and Y. Ni, Separation of hemicellulose and cellulose from wood pulp using a  $\gamma$ -valerolactone (GVL)/water mixture, *Sep. Purif. Technol.*, 2020, **248**, 117071.

53 A. Freyburger, *Novel Bio-Based Materials from Cellulose and Chitin dissertation*, University of Regensburg, 2018.

54 H. Q. Lê, J. Pokki, M. Borrega, P. Uusi-Kyyny, V. Alopaeus and H. Sixta, Chemical Recovery of  $\gamma$ -Valerolactone/Water Biorefinery, *Ind. Eng. Chem. Res.*, 2018, **57**(44), 15147–15158.

55 M. Granatier, H. Q. Le, Y. Ma, M. Rissanen, I. Schlapp-Hackls, D. Diment, *et al.*,  $\gamma$ -Valerolactone biorefinery: catalyzed birch fractionation and valorization of pulping streams with solvent recovery, *Helijon*, 2023, **9**, e17423.

56 D. J. G. P. Van Osch, L. J. B. M. Kollau, A. Van den Bruinhorst, S. Asikainen, M. A. A. Rocha and M. C. Kroon, Ionic liquids and deep eutectic solvents for lignocellulosic biomass fractionation, *Phys. Chem. Chem. Phys.*, 2017, **19**, 2636–2655.

57 A. M. Da Costa Lopes, K. G. João, A. R. Morais, E. Bogel-Lukasik and R. Bogel-Lukasik, Ionic liquids as a tool for lignocellulosic biomass fractionation, *Sustainable Chem. Processes*, 2013, **1**, 3.

58 M. Smuga-Kogut, D. Szymanowska-Powalowska, R. Markiewicz, T. Piskier and T. Kogut, Ionic liquid pretreatment of stinging nettle stems and giant miscanthus for bioethanol production, *Sci. Rep.*, 2021, **11**, 184565.

59 A. Brandt-Talbot, F. J. V. Gschwend, P. S. Fennell, T. M. Lammens, B. Tan, J. Weale, *et al.*, An economically viable ionic liquid for the fractionation of lignocellulosic biomass, *Green Chem.*, 2017, **19**, 3078–3102.

60 E. Husanu, A. Mero, J. G. Rivera, A. Mezzetta, J. C. Ruiz, F. D'Andrea, *et al.*, Exploiting deep eutectic solvents and ionic liquids for the valorization of chestnut shell waste, *ACS Sustain. Chem. Eng.*, 2020, **8**, 18386–18399.

61 M. Gholami, *Regeneration of Deep Eutectic Solvent Post Biomass Delignification [dissertation]*, University of Twente, 2024.

62 M. Jablonsky, A. Skulcova, L. Kamenska, M. Vrska and J. Sima, Deep eutectic solvents: fractionation of wheat straw, *Bioressearch*, 2015, **10**(4), 8039–8047.

63 S. Magalhaes, A. Moreira, R. Almeida, P. F. Cruz, L. Alves, C. Costa, *et al.*, Acacia wood fractionation using deep eutectic solvents: extraction, recovery, and characterization of the different fractions, *ACS Omega*, 2022, **7**, 26005–26014.

64 A. Mero, N. R. Moody, E. Husanu, A. Mezzetta, F. D'Andrea, C. S. Pomelli, *et al.*, Challenging DES and ILs in the valorization of food waste: a case study, *Front. Chem.*, 2023, **11**, 1270221.

65 Y. Liu, N. Deak, Z. Wang, H. Yu, L. Harneleers, E. Jurak, *et al.*, Tunable and functional deep eutectic solvents for lignocellulose valorization, *Nat. Commun.*, 2021, **12**, 5424.

66 J. L. Espinoza-Acosta, B. Ramirez-Wong, E. Carvajal-Millan, P. I. Torres-Chaves, B. Montano-Leyva and L. A. Bello-Perez, Ionic liquids and organic solvents for recovering lignin from lignocellulosic biomass, *Bioresearch*, 2014, **9**(2), 3660–3687.

67 L. G. Nair, K. Agrawal and P. Verma, Organosolv pretreatment: an in-depth purview of mechanics of the system, *Bioresour. Bioprocess.*, 2023, **10**, 50.

68 D. W. K. Chin, S. Lim, Y. L. Pang and M. K. Lam, Fundamental review of organosolv pretreatment and its challenges in emerging consolidated bioprocessing, *Biofuels. Bioprod. Bioref.*, 2020, **14**, 808–829.

69 M. Chen, F. Malaret, A. E. J. Firth, P. Verdia, A. R. Abouelela, Y. Chen, *et al.*, Design of a combined ionosolv-organosolv biomass fractionation process for biofuel production and high value-added lignin valorization, *Green Chem.*, 2020, **22**, 5161–5180.

70 D. W. K. Chin, S. Lim, Y. L. Pang, C. H. Lim, S. H. Shuit, K. M. Lee, *et al.*, Effects of organic solvents on the organosolv pretreatment of degraded empty fruit bunch for fractionation and lignin removal, *Sustainability*, 2021, **13**, 6757.

71 W. Lan, J. B. de Bueren and J. S. Luterbacher, Highly selective oxidation and depolymerization of  $\alpha$ ,  $\gamma$ -diol-protected lignin, *Angew. Chem., Int. Ed.*, 2019, **58**, 2649–2654.

72 F. Lu, C. Wang, M. Chen, F. Yue and J. Ralph, A facile spectroscopic method for measuring lignin content in lignocellulosic biomass, *Green Chem.*, 2021, **23**, 5106–5112.

73 Y. Chu and X. He, MoDoop: an automated computational approach for COSMO-RS prediction of biopolymers in ionic liquids, *ACS Omega*, 2019, **4**(1), 1–12.

74 A. Casas, S. Omar, J. Palomar, M. Oliet, M. V. Alonso and F. Rodriguez, Relation between differential solubility of cellulose and lignin in ionic liquids and activity coefficients, *RSC Adv.*, 2013, **3**(10), 3453–3460.

75 S.-T. Lin and S. I. Sandler, A priori phase equilibrium prediction from a segment contribution solvation model, *Ind. Eng. Chem. Res.*, 2002, **41**(5), 899–913.

76 C.-M. Hsieh, S. I. Sandler and S.-T. Lin, Improvements of COSMO-SAC for vapor-liquid and liquid-liquid



equilibrium predictions, *Fluid Phase Equilib.*, 2010, **297**(1), 90–97.

77 I. H. Bell, E. Mickoleit, C.-M. Hsieh, S.-T. Lin, J. Vrabec, C. Breitkopf, *et al.*, *J. Chem. Theory Comput.*, 2020, **16**(4), 2635–2646.

78 M. Mohan, B. A. Simmons, K. L. Sale and S. Singh, Multiscale molecular simulations for the solvation of lignin in ionic liquids, *Sci. Rep.*, 2023, **13**, 271.

79 I. Antolovic, J. Vrabec and M. Klajmon, COSMOPharm: Drug-polymer compatibility of pharmaceutical amorphous solid dispersions from COSMO-SAC, *Mol. Pharmaceutics*, 2024, **21**(9), 4395–4415.

80 M. Klajmon, Purely predicting the pharmaceutical solubility: what to expect from PC-SAFT and COSMO-RS?, *Mol. Pharmaceutics*, 2022, **19**(11), 4212–4232.

81 M. Mohan, K. L. Sale, R. S. Kalb, B. A. Simmons, J. M. Gladden and S. Singh, Multiscale molecular simulation strategies for understanding the delignification mechanism of biomass in cyrene, *ACS Sustain. Chem. Eng.*, 2022, **10**(33), 11016–11029.

82 N. Kumar, B. R. Taylor, V. Chourasia, A. Rodriguez, J. M. Gladden, B. A. Simmons, H. Choudhary and K. L. Sale, Multi-scale computational screening and mechanistic insights of cyclic amines as solvents for improved lignocellulosic biomass processing, *Green Chem.*, 2025, **27**, 5482–5497.

83 S. Wang, Y. Li, X. Wen, Z. Fang, X. Zheng, J. Di, H. Li, C. Li and J. Fang, Experimental and theoretical study on the catalytic degradation of lignin by temperature-responsive deep eutectic solvents, *Ind. Crops Prod.*, 2022, **177**, 114430.

84 L. Zhou, X. Liu, J. Zhang, Q. Li, M. Yuan and Z. Kang, Ionic liquid screening for lignocellulosic biomass fractionation: COSMO-RS prediction and experimental verification, *J. Mol. Liq.*, 2024, **407**, 125214.

85 M. J. Frisch, G. W. Trucks, H. B. Schlegel, G. E. Scuseria, M. A. Robb and J. R. Cheeseman, *et al.*, *Gaussian 16 (Revision C.01)*, Gaussian, Inc., Pittsburgh, PA, 2016.

86 M. Cossi, N. Rega, G. Scalmani and V. Barone, Energies, structures, and electronic properties of molecules in solution with the C-PCM solvation model, *J. Comput. Chem.*, 2003, **24**(6), 669–681.

87 S. Riniker and G. A. Landrum, Better informed distance geometry: using what we know to improve conformation generation, *J. Chem. Inf. Model.*, 2015, **55**(12), 2562–2574.

88 T. A. Halgren, Merck molecular force field. I. Basis, form, scope, parameterization, and performance of MMFF94, *J. Comput. Chem.*, 1996, **17**(5–6), 490–519.

89 RDKit: Open-source cheminformatics (release 2024\_09\_6), <https://www.rdkit.org>.

90 M. J. Abraham, T. Murtola, R. Schulz, S. Páll, J. C. Smith, B. Hess, *et al.*, GROMACS: high performance molecular simulations through multi-level parallelism from laptops to supercomputers, *SoftwareX*, 2015, **1**–2, 19–25.

91 J. Wang, R. M. Wolf, J. W. Caldwell, P. A. Kollman and D. A. Case, Development and testing of a general amber force field, *J. Comput. Chem.*, 2004, **25**(9), 1157–1174.

92 W. D. Cornell, P. Cieplak, C. I. Bayly, I. R. Gould, K. M. Merz, D. M. Ferguson, *et al.*, A second generation force field for the simulation of proteins, nucleic acids, and organic molecules, *J. Am. Chem. Soc.*, 1995, **117**(19), 5179–5197.

93 M. J. Frisch, G. W. Trucks, H. B. Schlegel, G. E. Scuseria, M. A. Robb and J. R. Cheeseman *et al.*, *Gaussian 09 (Revision A.02)*, Gaussian, Inc., Pittsburgh, PA, 2016.

94 J. L. F. Abascal and C. Vega, A general purpose model for the condensed phases of water: TIP4P/2005, *J. Chem. Phys.*, 2005, **123**(23), 234505.

95 G. Bussi, D. Donadio and M. Parrinello, Canonical sampling through velocity rescaling, *J. Chem. Phys.*, 2007, **126**(1), 014101.

96 M. Bernetti and G. Bussi, Pressure control using stochastic cell rescaling, *J. Chem. Phys.*, 2020, **153**(11), 114107.

97 B. Hess, P-LINCS: a parallel linear constraint solver for molecular simulation, *J. Chem. Theory Comput.*, 2008, **4**(1), 116–122.

98 U. Essmann, L. Perera, M. L. Berkowitz, T. Darden, H. Lee and L. G. Pedersen, A smooth particle mesh Ewald method, *J. Chem. Phys.*, 1995, **103**(19), 8577–8593.

99 L. Martinez, R. Andrade, E. G. Birgin and J. M. Martinez, PACKMOL: A package for building initial configurations for molecular dynamics simulations, *J. Comput. Chem.*, 2009, **30**(13), 2157–2164.

100 J. Polák, D. Ondo and J. Heyda, Thermodynamics of *N*-Isopropylacrylamide in water: insights from experiments, simulations, and Kirkwood-Buff analysis teamwork, *J. Phys. Chem. B*, 2020, **124**(12), 2495–2504.

101 H. Q. Lé, A. Zaitseva, J.-P. Pokki, M. Stahl, V. Alopaeus and H. Sixta, Solubility of organosolv lignin in  $\gamma$ -valerolactone/water binary mixtures, *ChemSusChem*, 2016, **9**(20), 2939–2947.

102 M. C. Barbu, T. Sepperer, E. M. Tudor and A. Petutschnigg, Walnut and hazelnut shells: untapped industrial resources and their suitability in lignocellulosic composites, *Appl. Sci.*, 2020, **10**, 6340.

103 S. Zhao, J. Nia, L. Yun, K. Liu, S. Wang, J. Wen, *et al.*, The relationship among the structural, cellular, and physical properties of walnut shells, *HortScience*, 2019, **54**(2), 275–281.

104 P. Sannigrahi, A. J. Ragauskas and S. J. Miller, Lignin structural modifications resulting from ethanol organosolv treatment of loblolly pine, *Energy Fuels*, 2010, **24**, 683–689.

105 J. S. Luterbacher, J. M. Rand, D. M. Alonso, J. Han, J. T. Youngquist, C. T. Maravelias, *et al.*, Nonenzymatic sugar production from biomass using biomass-derived  $\gamma$ -valerolactone, *Science*, 2014, **343**(6168), 277–280.

106 D. M. Alonso, S. H. Hakim, S. Zhou, W. Won, O. Hosseini, J. Tao, *et al.*, Increasing the revenue from lignocellulosic biomass: maximizing feedstock utilization, *Sci. Adv.*, 2017, **3**, e1603301.

107 I. T. Horvath, H. Mehdi, V. Fabos, L. Boda and L. T. Mika,  $\gamma$ -Valerolactone – a sustainable liquid for energy and carbon-based chemicals, *Green Chem.*, 2008, **10**, 238–242.



108 Y.-H. P. Zhang and L. R. Lynd, Toward an aggregated understanding of enzymatic hydrolysis of cellulose: noncomplexed cellulase systems, *Biotechnol. Bioeng.*, 2004, **88**(7), 797–824.

109 Y. Pu, F. Hu, B. H. Davison and A. J. Ragauskas, Assessing the molecular structure basis for biomass recalcitrance during dilute acid and hydrothermal pretreatments, *Biotechnol. Biofuels*, 2013, **6**, 15.

110 F. A. Carey and R. J. Sundberg, *Advanced Organic Chemistry, Part A: Structure and Mechanisms*, 5th edn, Springer, 2007.

111 J. L. L. N'Guessan, B. F. Niamké, N. J. C. Yao and N. Amusant, Wood extractives: Main families, functional properties, fields of application and interest of wood waste, *For. Prod. J.*, 2023, **73**(3), 194–208.

112 A. Chemat, M. Schweiger, D. Touraud, R. Müller, L. Lajoie, J. B. Mazzitelli, *et al.*, Cascade extractions of coffee silverskin: towards zero solid waste valorization of a byproduct, *Sustainable Chem. Pharm.*, 2024, **42**, 101779.

113 L. Dehne, C. V. Babarro, B. Saake and K. U. Schwarz, Influence of lignin source and esterification on properties of lignin-polyethylene blends, *Ind. Crops Prod.*, 2016, **86**, 320–328.

114 R. N. Nishide, J. H. Truong and M. M. Abu-Omar, Organosolv fractionation of walnut shell biomass to isolate lignocellulosic components for chemical upgrading of lignin to aromatics, *ACS Omega*, 2021, **6**, 8142–8150.

115 R. Protz, A. Lehmann, J. Ganster and H. Pink, Solubility and spinnability of cellulose-lignin blends in aqueous NMMO, *Carbohydr. Polym.*, 2021, **251**, 117027.

116 H. Nawaz, A. He, Z. Wu, X. Wang, Y. Jiang, A. Ullah, *et al.*, Revisiting various mechanistic approaches for cellulose dissolution in different solvent systems: a comprehensive review, *Int. J. Biol. Macromol.*, 2024, **273**, 133012.

117 X. Li, X. Yuan, G. Xia, J. Liang, C. Liu, Z. Wang, *et al.*, Catalytic production of  $\gamma$ -valerolactone from xylose over delaminated Zr-Al-SCM-1 zeolite *via* a cascade process, *J. Catal.*, 2020, **392**, 175–185.

118 L. Xiao, W. Liu, J. Huang, H. Lou and X. Qiu, Study on the antioxidant activity of lignin and its application performance in SBS elastomer, *Ind. Eng. Chem. Res.*, 2020, **60**(1), 1–12.

119 B. Wang, S.-F. Wang, S. S. Lam, C. Sonne, T.-Q. Yuan, G.-Y. Song, *et al.*, A review on production of lignin-based flocculants: sustainable feedstock and low carbon footprint applications, *Renewable Sustainable Energy Rev.*, 2020, **134**, 110384.

120 G. Foyer, B.-H. Chenfi, B. Boutevin, S. Caillol and G. David, New method for the synthesis of formaldehyde-free phenolic resins from lignin-based aldehyde precursors, *Eur. Polym. J.*, 2016, **74**, 296–309.

121 Y. Meng, Y. Cheng, J. Lu and H. Wang, A review on lignin-based phenolic resin adhesive, *Macromol. Chem. Phys.*, 2022, **223**, 2100434.

122 T. Ren, Z. Zhang, S. You, W. Qi, R. Su and Z. He, Isolation and purification of 4-propylguaiacol and 4-propylsyringol by extraction and crystallization from the products of reductive catalytic fractionation processes, *Green Chem.*, 2022, **24**(19), 7355–7361.

123 Y. Li, J. Zhu, Z. Zhang and Y. Qu, Preparation of syringaldehyde from lignin by catalytic oxidation of perovskite-type oxides, *ACS Omega*, 2020, **5**(5), 2107–2113.

124 K. Li, W. Zhong, P. Li, J. Ren, K. Jiang and W. Wu, Recent advances in lignin antioxidant: antioxidant mechanism, evaluation methods, influence factors and various applications, *Int. J. Biol. Macromol.*, 2023, **251**, 125992.

125 T. Heinze and T. Liebert, 10.05 – Cellulose and Polyoses/Hemicelluloses, in *Polymer Science: A Comprehensive Reference*, vol. 10, 2012, pp. 83–152.

126 T. Heinze and A. Koschella, Solvents applied in the field of cellulose chemistry: a mini review, *Polímeros*, 2005, **15**(2), 84–90.

127 S. Zhang, C. Chen, C. Duan, H. Hu, H. Li, J. Li, *et al.*, Regenerated cellulose by the Lyocell process, a brief review of the process and properties, *Bioresource*, 2018, **13**(2), 4577–4592.

128 C. Michels and B. Kosan, Lyocell process – material and technological restrictions, *Chem. Fibers Int.*, 2000, **50**, 556–561.

129 T. Rosenau and A. D. French, *N*-Methylmorpholine-*N*-oxide (NMMO): hazards in practice and pitfalls in theory, *Cellulose*, 2021, **28**, 5985–5990.

130 E. Hytönen, L. Sorsamäki, E. Kolehmainen, M. Sturm and N. V. Weymarn, Lyocell fibre production using NMMO – a simulation-based techno-economic analysis, *Bioresource*, 2023, **18**(3), 6384–6411.

131 M. Schweiger, T. Lang, E. Mueller, D. Touraud and W. Kunz, Influence of the biomass-source and the extraction process on lignin properties and  $\gamma$ -valerolactone induced conversion of biomass towards valuable lignin monomers, *RSC Sustainability*, 2025, DOI: [10.1039/d5su00324e](https://doi.org/10.1039/d5su00324e).

